

NSTX Upgrade

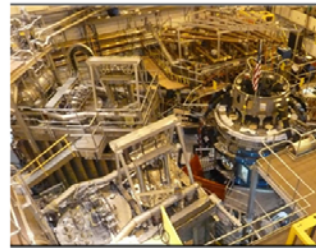
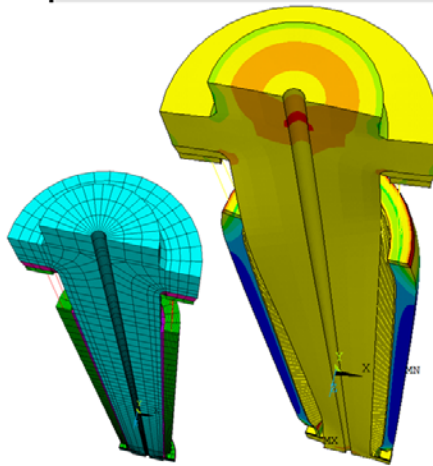
OH-TF Aquapour Interaction

NSTXU-CALC-133-16-00

June 2015



AquaCement Problem
 P. Titus, H. Zhang, A.
 Brooks, A. Khodak



<u>Prepared by P. Titus</u>	<u>Reviewed by I. Zatz</u>
<u>Section 10.0,11.0 Prepared by Han Zhang</u>	<u>Reviewed by P. Titus</u>
<u>Section 12.0 Prepared by A. Brooks</u>	<u>Reviewed by P. Titus</u>

PPPL Calculation Form

Calculation # NSTXU-CALC-133-16-00 Revision # 00 _____ WP #, 1672
(ENG-032)

Purpose of Calculation: (Define why the calculation is being performed.)

The purpose of this calculation is to assess effects of retaining the Aquapour material in what was to be a gap between the TF and OH coils. The calculation is also intended to identify the consequences of operation with frictional interaction between the OH and TF coils and to provide guidance on how to avoid frictional interaction. If frictional interaction is allowed in the future, this calculation provides some guidance on how it might be accommodated. Related to the Aquapour issue is qualification of operation at higher OH temperature, and possible loss in preload at an elevated temperature.

References (List any source of design information including computer program titles and revision levels.)

These are included in the body of the calculation, in section 6.3

Assumptions (Identify all assumptions made as part of this calculation.)

While some measurements have been made regarding the physical and electrical properties of the Aquapour, and these have been found acceptable, it is not characterized as rigorously as other coil materials. It is assumed that the long term properties and behavior will remain acceptable. It is assumed that the slip plane measured during heating tests during August and September 2014, is at the Teflon sheet surrounding the Aquapour.

Calculation (Calculation is either documented here or attached)

These are included in the body of the following document

Conclusion:

As of June 2015, the project approach is to develop operational controls, implemented in the DCPS to maintain the OH hotter than the TF to eliminate the possibility of interactions between the TF and OH coils. These calculations address the consequences of having frictional interactions that would result from the TF being hotter than the OH. The conclusion of this calculation is that tensile strains beyond the NSTX allowable would develop. Presently, no frictional interaction is allowed. In the future, to develop full performance, it may be considered. One possible "fix" to the problem is to allow hotter OH operation, biasing the OH operation temperatures warmer than previously planned to ease the ability to maintain the OH hotter than the TF Operation at 110C. Operation at 120 C is probably possible as well with some care to maintain the required preload in the OH stack. Operations at 110C and 120C will require some adjustments to the DCPS algorithms for the OH launching load.

Wires that were intended to facilitate Aquapour removal remain in place and don't pose any threat. But, if the Aquapour has voids or bubbles, it may be subject to progressive damage to its insulating properties by progressive partial discharges (see section 12.0). Mechanically, the Aquapour was tested (section 13.0) and is judged to be strong enough to stay in place. Mechanical design of the OH supports at the base will limit escape of crushed Aquapour, but inspections should be carried out in maintenance down times to check for dust or chips of Aquapour. Degradation of the OH and TF hipots should be tracked for the possibility that the Aquapour is degrading coil performance.

Cognizant Engineer's printed name, signature, and date

Steve Raftopolos _____

I have reviewed this calculation and, to my professional satisfaction, it is properly performed and correct.

Checker's printed name, signature, and date

Irving Zatz/Peter Titus _____

2.0 Table of Contents

Title Page	1.0
ENG-33 Forms	
Table of Contents	2.0
Revision Status Table	3.0
Executive Summary	4.0
Input to Digital Coil Protection System	5.0
Design Input,	
Criteria	6.1
References	6.2
Scenarios	6.3
OH and TF Current Only Scenario	6.1.1
12 (Bad) Scenarios	6.3.2
14 (Good) Scenarios	6.3.3
Materials and Allowables	6.4
Models	7.0
Model Used to Simulate Tests in the Coil Shop	7.1
Models Used to Simulate Frictional Interaction during Operation	7.2
Smeared OH Properties	7.3
Simulation of Heat-Up on the Winding Machine	8.0
Simulation of Frictional Interaction with OH Lorentz Loads Only (by P. Titus)	9.0
Effect of Preload Mechanism to Offset the Tensile Stress	9.1
Torsional Shear Stress in the OH if it is Frictionally Connected to the TF	9.2
Simulation of 14 (Bad) Equilibria Supplied by Stefan Gerhardt(by Han Zhang)	
Using (Titus) OH Load File	10.0
Simulation of 14 (Good) Equilibria Supplied by Stefan Gerhardt (by Han Zhang)	11.0
Simulation of 14 Equilibria with Full OH Loading	11.1
Simulation of 14 Equilibria with Full PF Loading	11.2
Electrostatic Analysis of Trapped Wires in Aquapour (A. Brooks)	12.0
Tensile Tests of “AquaCement” Material	13.0
Tensile Test Samples/ CTD Tensile Strain Tests	14.0
Creep Test Sampler/CTD Creep Tests	15.0
Appendix A Emails	

3.0 Revision Status Table

Rev 0	Initial Issue
-------	---------------

4.0 Executive Summary

Frictional interactions of the OH and TF were investigated early in the analyses of the OH coil. Ali Zolfaghari raised the concern in his OH coil calculations. Frictional interaction was also pointed out as a concern by MAST reviewers at one of the early NSTX-U peer reviews. Ali's discussion in his calculation follows:

“Thermally, the frictional interaction between the TF and OH coil "drags" the OH coil with the expanding TF and causes unacceptably large tensile stresses in the OH. This was found to be true even with a low friction material interface. Consequently, a gap between the two coils was intended to be introduced. This was to be accomplished through the use of a water soluble layer applied on the TF on which the OH was wound. Water jets were then used to attempt to remove the layer.”

As of July 2015, the Aquapour could not be removed, and measures have been taken to avoid the possibility of frictional interaction between the OH and TF by controlling their temperatures. Much of what follows is intended to show the difficulties that would have arisen if the interaction had been allowed, and to provide some guidance on how it might be allowed in future upgrades.

During the VPI, epoxy leaked past dams and impregnated the Aquapour. The Aquapour/epoxy material could not be dissolved with water. With the Aquapour left in the annular gap between the NSTX-U TF and OH, the coils would frictionally interact. Experience attempting to remove the material indicates that it is fairly strong. This was confirmed by tests by S. Jurczynski (See Section 13). It is assumed that the slip plane measured during heating tests, conducted in August and September 2014, is at the Teflon sheet surrounding the Aquapour. The tall narrow geometry of the coils provides a large cylindrical frictional surface for traction and relatively small cross sections to resist the frictional forces.

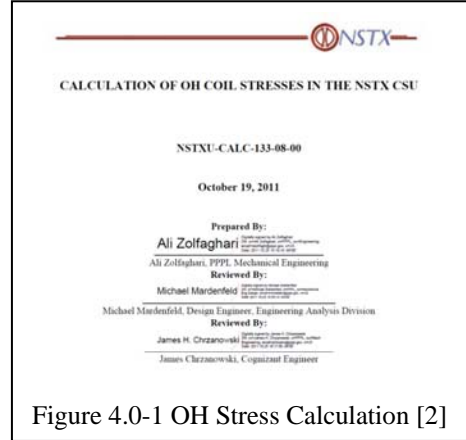


Figure 4.0-1 OH Stress Calculation [2]

Bond is broken, Aquapour is not Removed, OH Lorentz Forces Off , OH at 20C TF Ramped to 100C

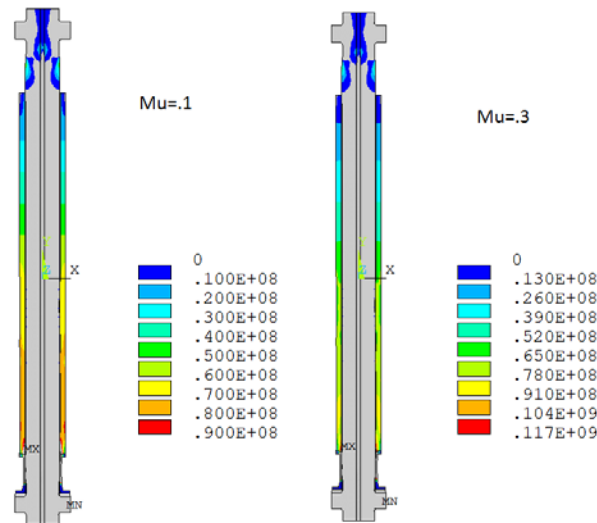


Figure 4.0-2 Showing a Worst Case Situation with the TF Hot and the OH Cold

This type of interaction between coils is not unheard of in tokamak design. The TF is bucked against the OH in the JET magnet design. A similar interface was used in one of the early ITER design concepts. Bucked and bucked / wedged configurations were investigated in CIT and BPX. The IGNITOR reactor concept relies on a bucked low friction interface between the OH and TF. Reliance on predictable frictional behavior puts some constraints on operation. ITER requires high wedging pressure and friction on the vaulted/wedged faces of the inner legs to support the out-of-plane loads generated by the poloidal fields. Operation with lower toroidal fields and high poloidal fields will be limited. Since the Aquapour has not been removed, NSTX-U will have to develop a means of selecting scenarios that produce acceptable interactions between the TF and OH. Early operating plans simply maintain the OH temperature above the TF temperature. The main difficulty arises from a cold OH and a warm TF. This can produce axial (vertical) tensile stresses in the OH as the TF expands radially and develops frictional loads and expands vertically which will tend to stretch the OH. The OH winding pack is not designed to take substantial axial (vertical) tension. If the OH is maintained at a higher temperature than the TF throughout the shot, significant frictional forces will not develop. This is not an absolute necessity. When energized, the OH expands slightly and relieves the radial pressure between the TF and OH, and thus relieves the frictional connection between the two coils. Cooler OH temperatures can be tolerated if the OH swing peak currents are timed to relieve the built up OH axial tensile stresses. Also, small tensile strains have been tested by CTD and found not to degrade the electrical properties of the coil. Future operations may allow some frictional interaction and the resulting tension in the OH coil.

In Figure 4.0-2, the tensile stress with no OH Lorentz forces applied produces ~100 MPa tension for a range of friction coefficients, for an 80 C temperature differential between OH and TF. If the OH is energized during the TF expansion, the tension stress drops to ~60 MPa. This is shown in Figure 4.0-3. These examples aren't representative of a typical plasma shot, but they are representative of a TF test shot. The first conclusion that can be drawn is that the TF test shots need to be revised. To investigate a plasma shot, an example scenario of OH and TF currents was provided by S. Gerhardt. This formed the basis for a series of analyses.

Bond is broken, Aquapour is not Removed, OH Lorentz Forces On , OH at 20C TF Ramped to 100C

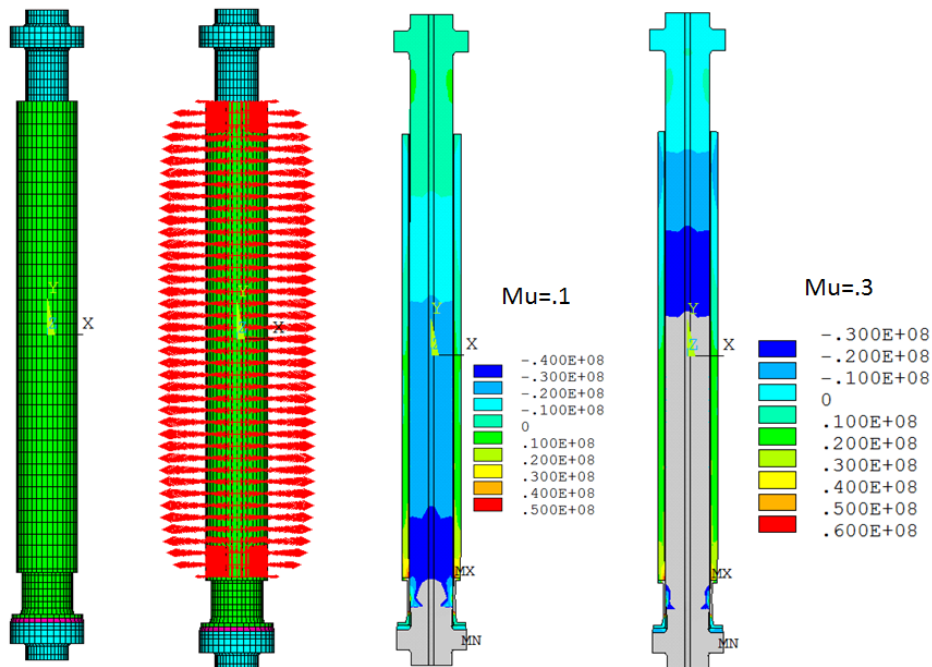


Figure 4.0-3 The OH is Energized During TF Expansion

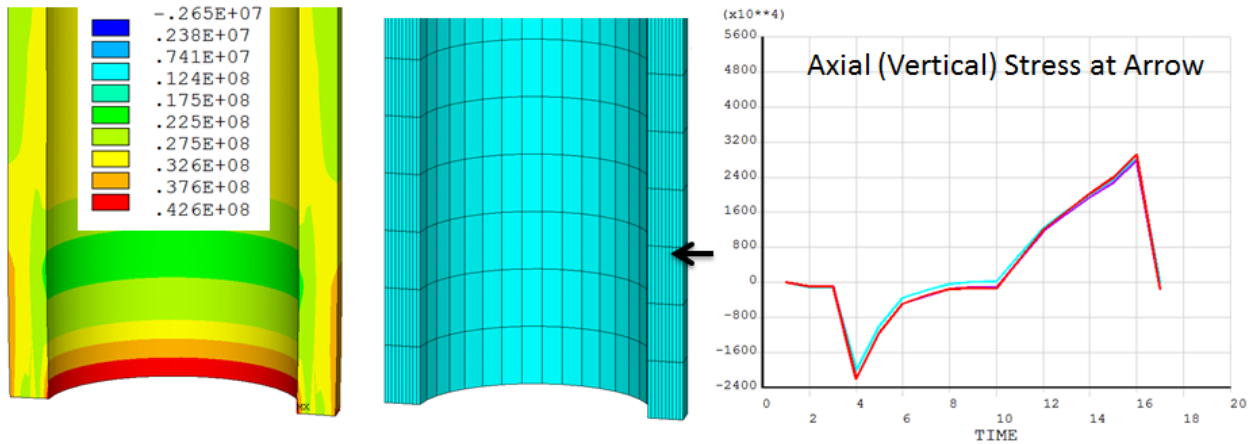


Figure 4.0-4 Axial Stress for a Specific Scenario, $\mu=.3$

In the simulation of the example scenario, the vertical tension is 27 MPa. The example scenario was then used with various OH and TF temperatures, assuming these could be obtained by starting the coils at different temperatures.

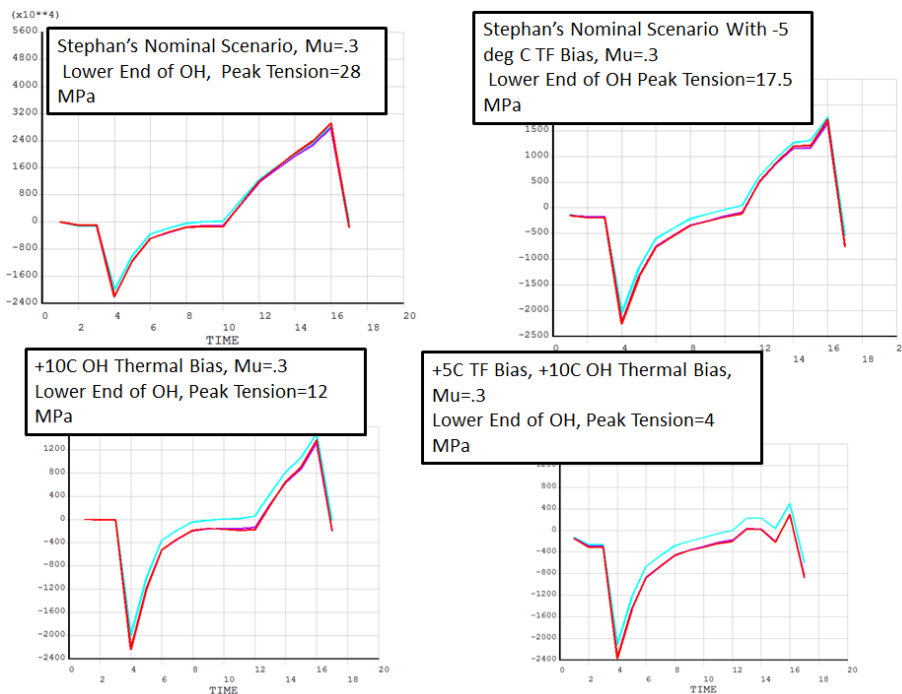


Figure 4.0-5 Axial Stress S. Gerhardt's Example Scenario with Varied OH and TF temperature biases, and a Friction Coefficient of .3

Figures 4.0-4 and 5 show analyses of the representative scenario and the effect of varying biases in the OH and TF coils. It is evident that the peak tension stress in the OH can be managed by increasing the OH temperature, lowering the TF temperature or both. With an allowed tension stress established, an allowed temperature differential could be established. As a part of the qualification of the CTD-425 epoxy system, tensile/adhesion tests were performed. The static and fatigue "Flatwise" tensile strength of the 425 system is about 15 Mpa (min) and the allowable would be half this. This was tested at 50C to qualify tensile stresses in the TF. However, the OH includes a Kapton wrap, which is essentially a parting plane. This would reduce the OH tensile strength to essentially zero. The winding pack would be able to survive small

tensile strains. The OH winding pack was tested for tensile strains expected in the post shot cooldown and this can be used for future qualification of some degree of frictional interaction between the coils. The tensile stress/strain vs temperature difference is needed to guide these scenarios and this worked out to about 1 MPa per 1 degree C. To obtain the tensile strain, this should be divided by the winding pack modulus used in the analysis, which in this case was 111GPa (note that better estimates of the modulus have been derived in the cooldown calc[8] and are discussed in section 7.3).

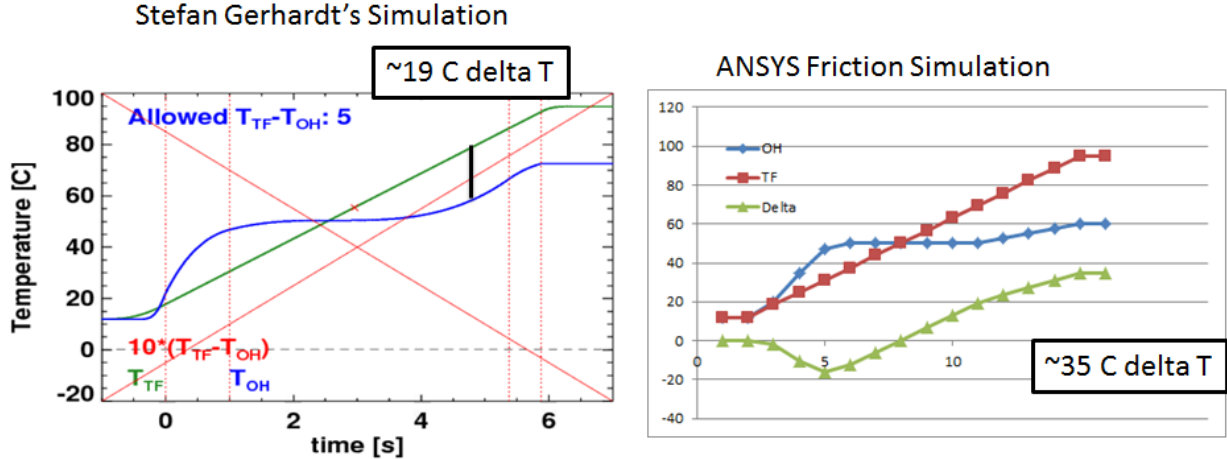


Figure 4.0-6 TF and OH Temperatures bt S. Gerhardt (left) and P Titus (right)

In figure 4.0-6, Gerhardt’s temperature differential of 19 C is lower than what was used in the ANSYS simulation. This should produce a vertical tensile stress of ~19 MPa based on the simple model results. It is more like 30 MPa in the ANSYS scenario simulation. This was basically an error in the input of the OH temperature in the ANSYS simulation. This is apparent in the OH temp plot in figure 4.0-5. The outcome of these studies is that a tensile strain of $1e6/100e9$ per degree that the OH is cooler then the TF can be expected.

The cross sections of TF and OH are comparable. The area of the TF cross section is $(0.194^2 \cdot \pi =) 0.1182m^2$ and the area of the OH cross section is $(.0655m^2 \cdot \pi \cdot .243m =) .1 m^2$. So if they were locked, the TF thermal expansion strain would be split between OH and TF. And crudely, the stress would be $E \cdot \text{Alpha} \cdot \text{delta T} / 2 = 111e9 \cdot 17e-7 \cdot 35 / 2 = 33 \text{ MPa}$. Possibly, it is behaving more like it is locked than sliding.

Another possible source of tensile strain is the solenoidal centering load. With an OH free from interaction with the TF, the axial loads in the ends of the coil would produce only compressive stresses that accumulate towards the middle of the coil. If the coil ends are restrained by friction, the centering Lorentz forces could appear as tension just inside the upper and lower ends of the OH.

The scenario simulation was re-run with a bias on the OH temperature of 10 degrees and a TF bias of 5 degrees. The OH bias would be accomplished by a flux bias of the OH that increases its currents. The TF bias would be accomplished by cooling the TF temperature below the 12C that is currently planned. With these two thermal adjustments, the tensile stress dropped to 4 MPa, shown in Figure 4.0-5 lower right.

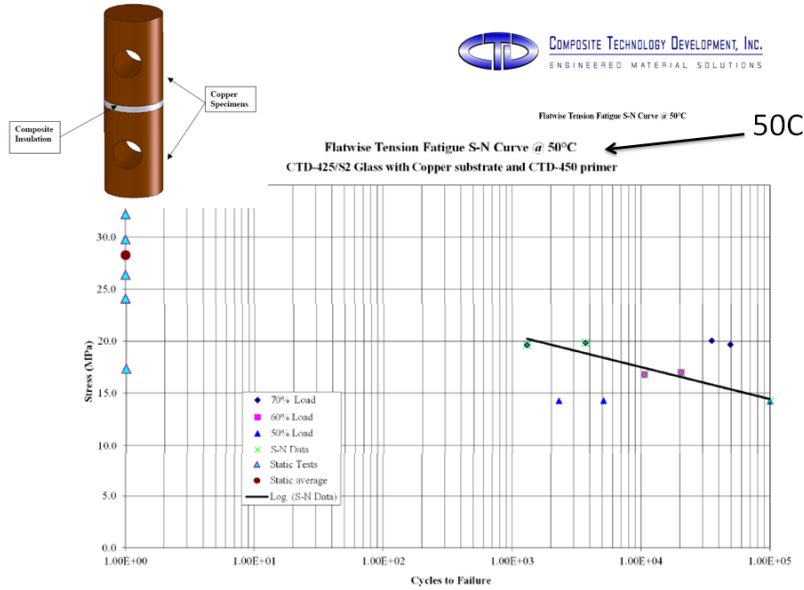


Figure 4.0-7 TF CTD Tension Tests for the CTD-425 system (with CTD 450 primer) adhered to copper. With no Kapton – Intended to simulate the TF Insulation Geometry

Without the Kapton, based on tensile tests for the TF system, an allowed tensile stress would be half the 15 MPa tensile strength in fatigue shown in Figure 4.0-6. Without Kapton, the static or low cycle tensile strength actually is in the 20 to 35 MPa range. Inclusion of Kapton reduces the tensile capacity to near zero. This was found in the MIT tests done on ITER insulation and in the CTD Array Tensile Strain Tests [13]. Using an allowable tensile strain, an allowed temperature differential can be developed, and this can be estimated either from the earlier NSTX performance or by strain controlled fatigue tests.

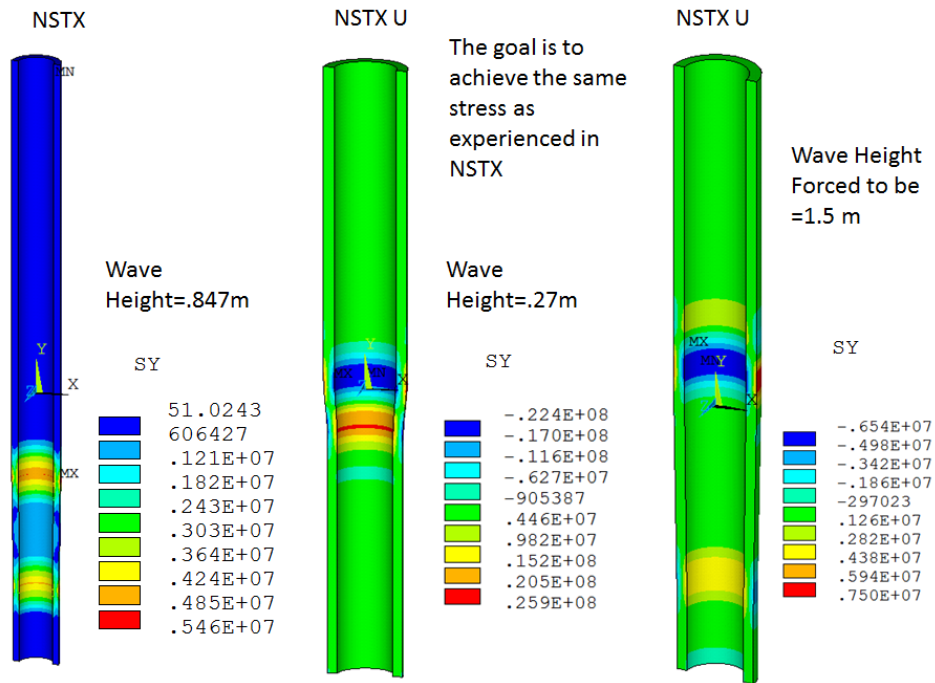


Figure 4.0-8 Comparison of Cooldown tensile stresses in NSTX and NSTX-U, Ref [8]

The NSTX – NSTX-U comparison was treated in the context of the wave cooling concern. This is addressed in calculation NSTXU-CALC-133-17-0 “NSTX Upgrade OH Cooldown System and Preheater” [8]. NSTX operated successfully with many cooldown cycles that would produce a stress in the coil of around 5 MPa. While the insulation systems are different, with the addition of Kapton, the expectation is that the Upgrade OH coil would be OK with the same strains as experienced by the original NSTX. This would set the allowable to 5MPa. The winding pack was tested by CTD in December 2014[13] and this has established a proper tensile strain allowable.

A more predictive rule for limiting the tensile strains was desired – applicable to more scenarios than the one example provided. The TF/OH model with the frictional interface was run with friction coefficients of .1 and .3. The peak tensile stress at the bottom of the OH and the tensile stress about ½ meter from the bottom are tabulated below, in Figure 4.0-9. For this study, No Lorentz forces are included in either the TF or OH. The OH temperature is held constant, and then TF temperature increase is ramped. The ½ meter height was chosen because the local tensile strains and shear stresses at the base of the OH are governed mostly by the cooldown thermal loads and were qualified in reference [14].

The TF/OH model with the frictional interface was run with friction coefficients of .1 and .3. The peak tensile stress at the bottom of the OH and the tensile stress about ½ meter from the bottom are tabulated at right. For this study, No Lorentz forces are included in either the TF or OH. The OH temperature is held constant, and then TF temperature increase is ramped.

Stefan Provided Han with 14 Scenarios with different OH biases and TF-OH temperature differentials. OH tensile stress about ½ meter from the bottom is tabulated at right. For this study, OH Lorentz forces are included.

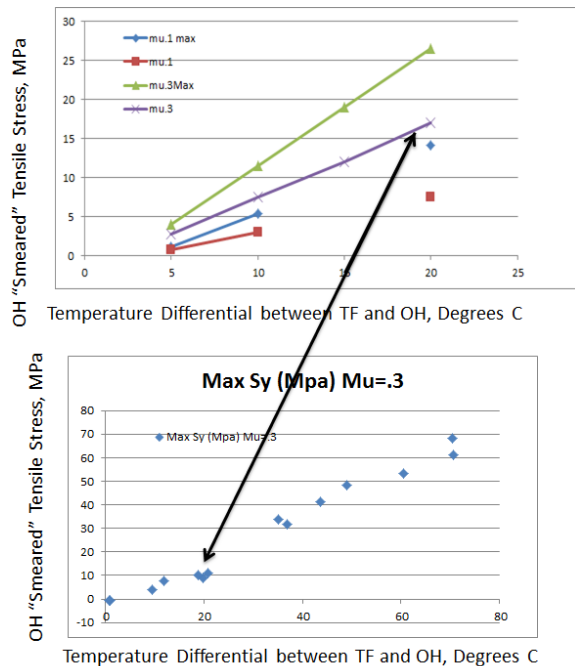


Figure 4.0-9 Tensile Stress vs. TF-OH Differential Temperature

This simulation in the top of Figure 4.0-9 was artificial in that it simply ramped the TF temperature. It shows the sensitivity to the friction coefficient. A friction coefficient of .1 is expected because there is a Teflon sheet between the TF and OH, but a more conservative treatment of the uncertain interface formed by the aquacement, is wise. Stefan Gerhardt provided scenarios that had a variety of differences in OH to TF temperature, and were “real” scenarios, in that they simulated initiation and a plasma pulse. The lower plot in Figure 4.0-9 is by Han Zhang based on Stefan’s data and is for mu=.3. In the upper mu=.3 plot, at 20 degrees differential temperature, 17 MPa tension would be expected. In Hans lower plot, 10 to 15 MPa would be expected. Both of these plots suggest a simple rule of thumb that you get about 1 MPa tension for each degree of temperature difference, and 1e6/111GPa tensile strain per degree that the TF is hotter than the OH.

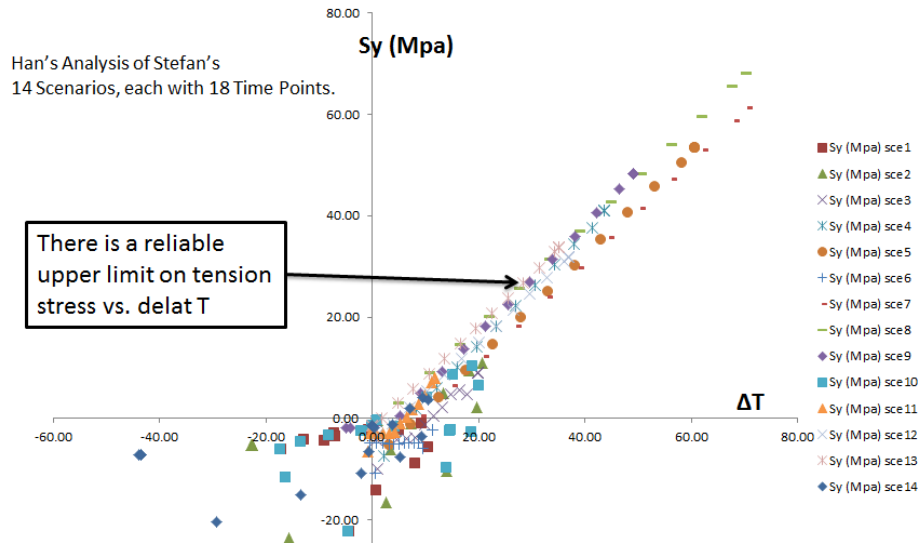


Figure 4.0-10 Vertical Tension Stress for 14 Scenarios vs. Temperature Difference Each for 18 Intermediate Time Points.

Figure 4.0-10 shows that for many simulations, there is a reliable upper bound on the tensile stress of 1 MPa (Tensile Strain of 1MPa/111GPa) per degree that the TF is hotter than the OH. This is true for intermediate time points within scenarios as well as for the variety of scenarios simulated.

So, for a 5 MPa allowable, a 5C temperature differential should cover the uncertainty in friction coefficient. The Teflon parting plane in the interface between the TF and OH would be deemed appropriate to produce a friction coefficient of approximately .1. For this value of mu, the allowed temperature differential would be more like 10 degrees C. For specific scenarios which utilize the OH and produce Lorentz forces, friction forces due to higher temperature differentials would be relieved. Analysis of specific scenarios is path dependent, but Zhang's simulations support a simpler limit based on the differential temperature. The DCPS now has the capability of tracking the temperature difference between coils during the shot. One of Stefan Gerhardt's slides describing Han's bounding curves is included below.

Analysis Supports the Use of Temperature Differentials for The Initial Protection Scheme: Method

- Created 14 different discharge scenarios.
 - Mostly 2 MA, 1T, but a few at lower field and current.
 - Many variations in the pre-charge and pre-heat.
 - All had the TF temperature eventually exceed the OH temperature, sometimes by a large amount.
 - So are useful for defining protection scheme.
 - Had a wide range of OH states during the time when T_{TF} exceeded T_{OH} by 0-10 C.
- Used ANSYS to analyze the OH stress at 18 times in each of the discharge scenarios.
 - 14x18=252 combinations of stress, temperature difference, OH state
- Motivation: Find a bounding curve for the OH stress that is a function of only the temperature difference.

Figure 4.0-11 Figure from S. Gerhardt's Presentation [3]

Note that while there appears to be an allowable degree to which the TF can be hotter than the OH. The present (June 2015) limitation on operation is set to avoid any situation in which the TF is hotter than the OH. In the future, with the availability of the CTD tensile strain test results, some degree of adverse differential temperatures may be allowed.

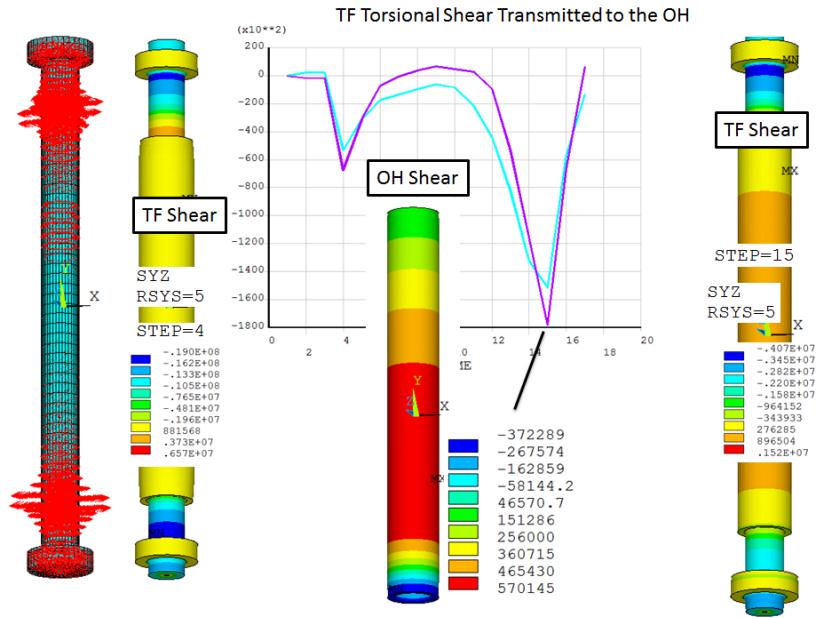


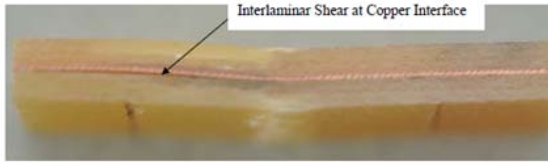
Figure 4.0-12 TF Torsional Shear Transmission to the OH

TF Torsional shear transmission to the OH was investigated. This was not found to be significant. Figure 4.0-12 shows the results of a scenario simulation in which there was significant interaction between the TF and OH. The torsional stress imposed on the OH was .5 MPa. The fatigue limit in the TF insulation system is 25 MPa. The Kapton in the OH system will reduce this, but in other interleaved glass-Kapton systems like the ITER CS, the shear strength is significantly greater than .5 MPa. This conclusion is scenario dependent, and adds some complexity to what will have to be considered if frictional interactions between the coils are to be allowed. It is conceivable that if interactions are allowed, a small torsional shear could occur where there are some otherwise acceptable tensile strains. The present approach is to avoid this by disallowing the frictional interactions.

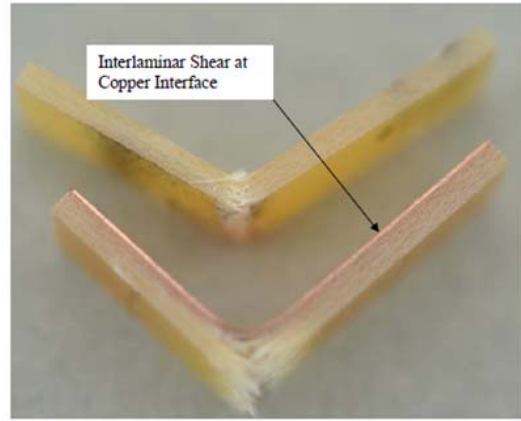
So far, the tensile allowable is based on not allowing any de-lamination or de-bonding at the copper- epoxy interface. It is actually very common to have conductors de-bond from the copper and delaminate at Kapton interfaces. Kapton is included in the insulation system to provide a reliable electrical barrier even when small cracks develop in the insulation. Its inclusion in the winding pack increases the likelihood of delamination but drastically diminishes the negative consequences. Kapton has a large % elongation (150%) at room temperature that can absorb local strains near cracks without electrical failures. ITER uses a system with Kapton in the winding pack and has shown good electrical performance with local tensile stresses larger than those expected in NSTX.

If there is Tensile or Shear Failure, It is desirable to have debonding at the Copper /Insulator Interface.

The photos are From the NSTX CTD 425 Fatigue Qualification:



CTD-425 Specimen #15- Fatigue at 60% of Ultimate Stress (31 MPa, 21867 cycles)



CTD-425 Specimen #14- Fatigue at 60% of Ultimate Stress (31 MPa, 26851 cycles)

Figure 4.0-13 TF Insulation Samples after Cyclic Failure

One requirement in the NSTX TF insulation qualification tests was that the epoxy system – even with a good primer – should break-away cleanly from the conductor when the epoxy failed. Figure 4.0-13 shows the failure in the short beam shear test in which the bond to copper separated cleanly. This was typical of the breaks that established the load rating of the insulation. This behavior is even more reliable at the Kapton tape interfaces. Figure 4.0-14 shows the separation of a conductor from the array sample used in the CTD tensile strain tests. The parting plane at the Kapton leaves “shells” without through cracks of barrier insulation even after delamination.

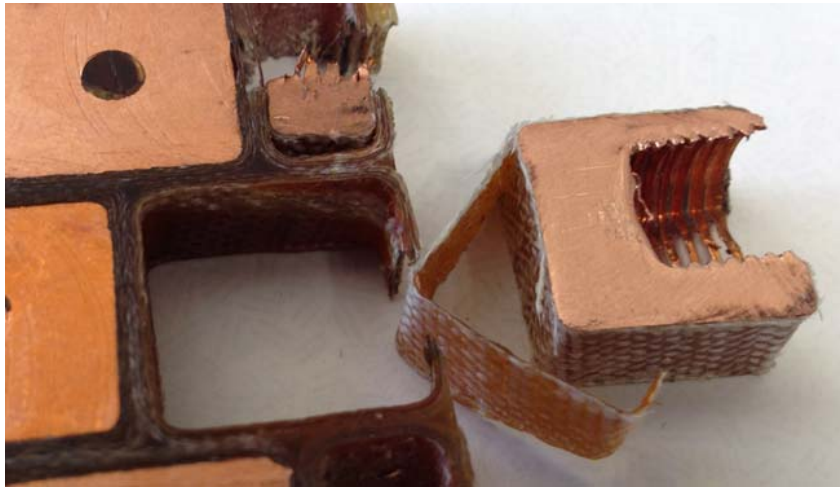


Figure 4.0-14 Separation of a Conductor in the CTD Array Test Specimen

To simulate the effects of de-bonding, a model that includes the conductor and insulation details was developed. The model is shown in Figure 4.0-15.

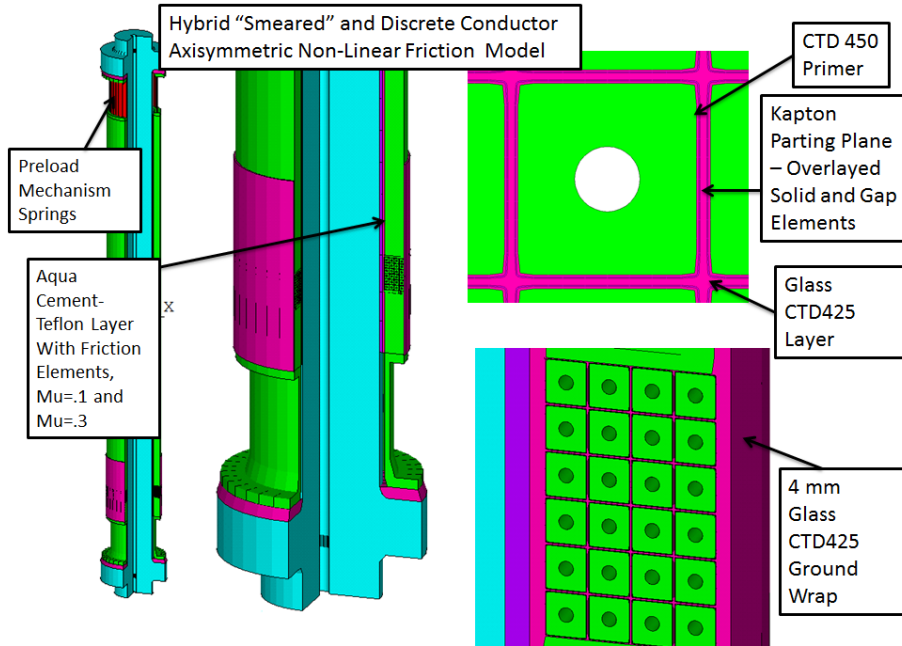
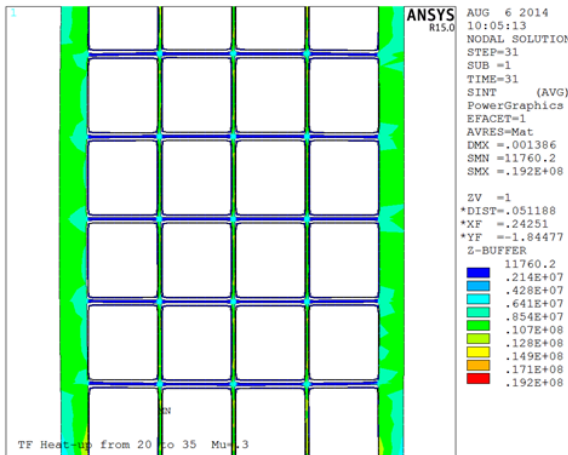


Figure 4.0-15 Hybrid "Smeared" Winding Pack Model with a region of Discrete Conductors



For a 15 degree Delta T, Which should produce 15 Mpa Tension, the two Kapton Layers Modeled with Gap Elements, Open Up $(.135e-3--.126e-3) * 39.37 = .000354$ inches, or $.000177$ inches per Kapton Layer, and the ground wrap sees ~ 10 Mpa tension in its strong dimension.

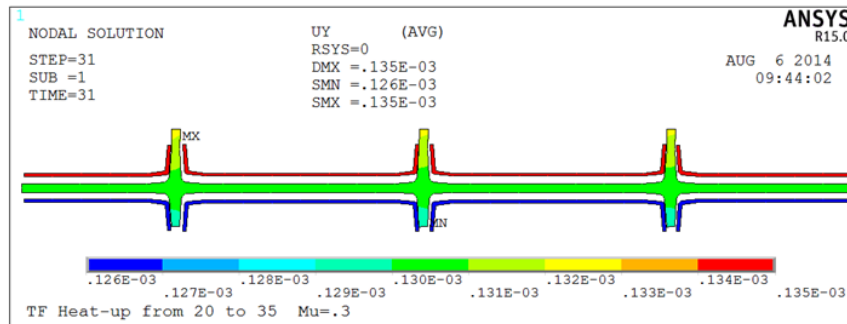


Figure 4.0-16 Gap Openings between Kapton Layers

From Figure 4.0-16, for a 15 degree delta T, which should produce 15 MPa tension, the two Kapton layers modeled with gap element interfaces open up $(.135e-3 - .126e-3) * 39.37 = .000354$ inches or .000177 inches per Kapton layer and the ground wrap sees ~10 MPa in its strong direction. With displacements this small it is hard to imagine that the insulation system would be damaged by these small strains. The only way to qualify these strains is by a test – similar to the ITER array test, but the NSTX test is tensile. CTD was contracted to do a tensile strain controlled test. The specified strain was $4.0e-4$. The actual strain imposed in the tests was closer to $6e-4$ (Figure 4.0-17). This would correspond to a tensile stress in the Aquapour simulations of $111e9 * 4e-4 = 44.4$ to 66 MPa. In the simulations shown in figure 4.0-15 and 16, the tensile strain in the conductor winding pack can be estimated from the tensile strain in the ground wrap of $10 \text{ MPa} / 20 \text{ GPa} = 5e-4$.

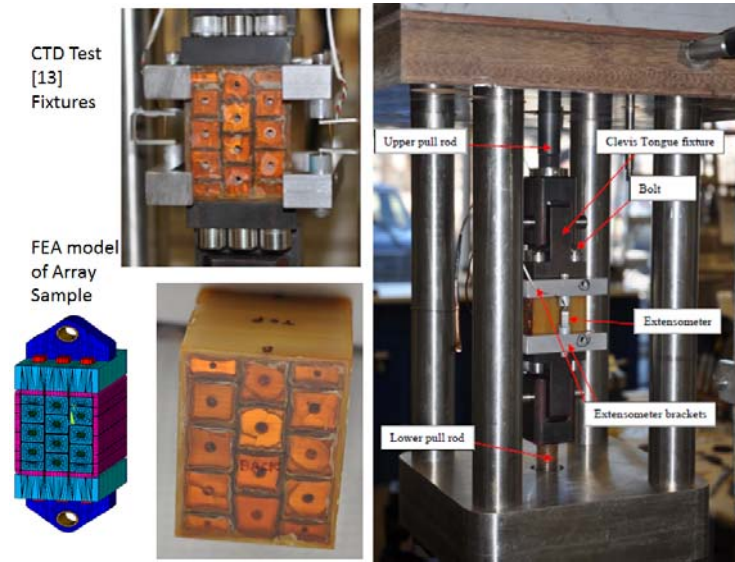


Figure 4.0-17 Test Specimen [13]

As of June 2015, the project approach is to maintain the OH always hotter than the TF coil. This constraint has been built into the Digital Coil Protection System (DCPS). Simulations of the frictional interaction between the coils are academic as long as the OH can be maintained hotter than the TF. It will be easier to keep the OH hotter than the TF if the allowable temperature limit for the OH can be increased from 100C.

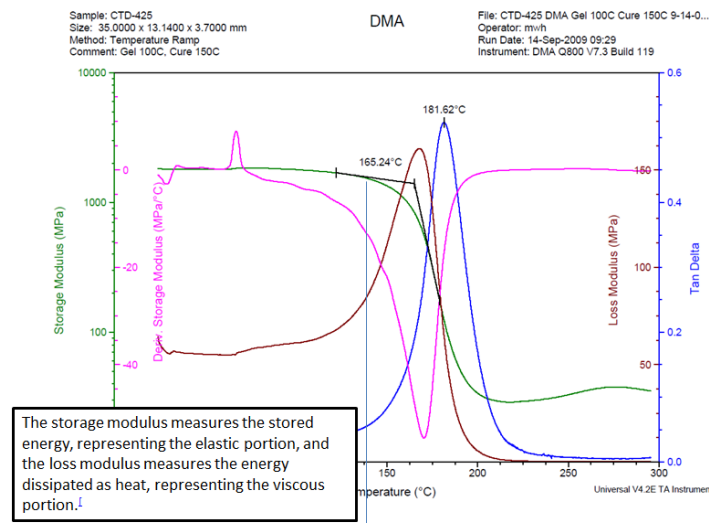


Figure 4.0-18 Storage Modulus Plots Indicating the Glass Transition Temp

In Figure 4.0-18 the storage modulus plot is a measure of when the epoxy system shifts from an elastic to a plastic material. This occurs at the glass transition temperature and is around 170 C in this plot – the same as the cure temperature. Qualification of a load carrying capacity at 170 C is not possible. The temperature dependent compressive strength of the CTD-425 material, and the creep behavior as a result of time-temperature and load is addressed in more detail in section 15.0

Selective choice of scenarios and preheat of the OH for non-inductive scenarios allows maintenance of the OH temperature above the TF. This has been presented by Stefan Gerhardt and Jon Menard (during the December 2014 Readiness Review) as allowing a full physics program for NSTX-U. Access to long pulse experiments would be aided by the ability to operate the OH at temperatures higher than 100C. The glass transition temperature of the CTD 425 system is above 135C but there is some indication that it is starting to soften. Samples have been tested at 110C and 120C to evaluate if the creep behavior at these temperatures might cause loss of preload in the OH coil.

What Happens if the OH is Allowed to Operate up to 110 C? 1: Kinder Operating Window

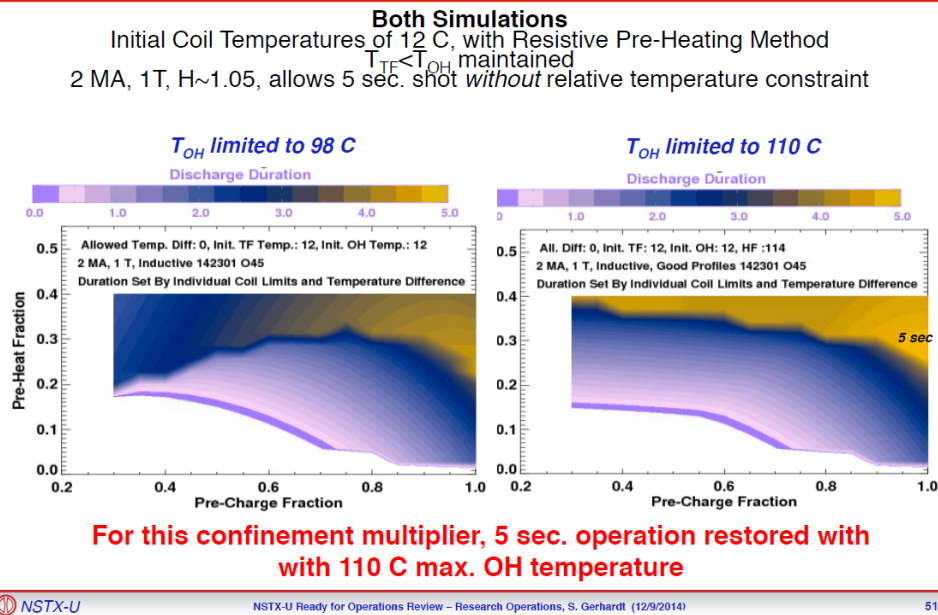


Figure 4.0-19 Improved operating Window with 110 Allowed OH Temperature

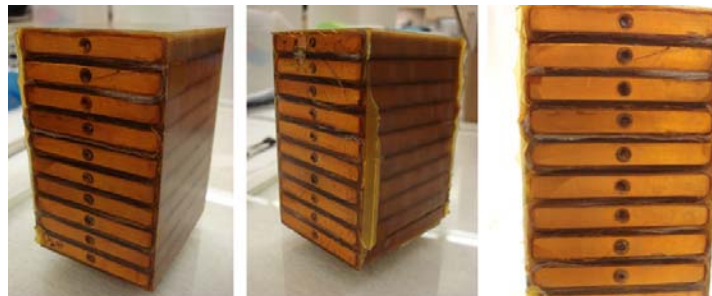
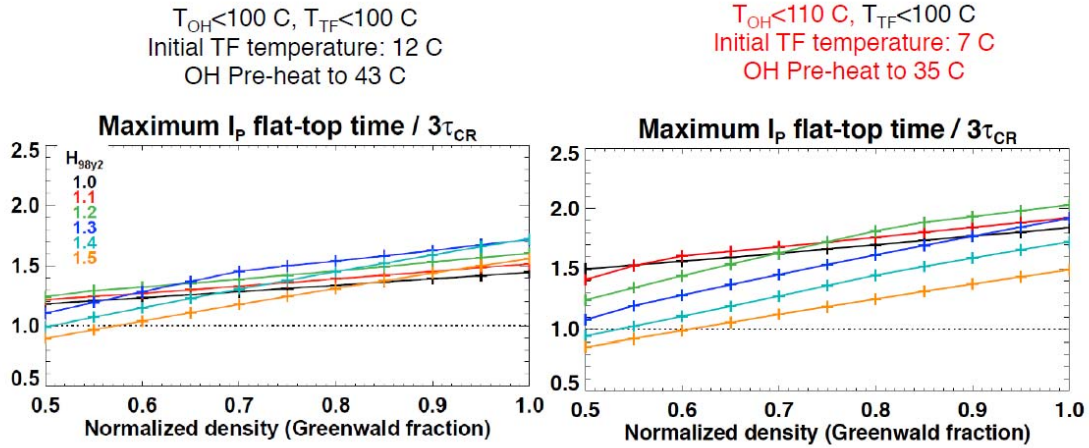


Figure 4.0-20 CTD Creep Test Specimen

In Section 15, the effect of creep on the OH preload is addressed. Creep has the effect of decreasing the preload from a nominal minimum of 20,000 lbs to 15,000 lbs for 110C peak temperatures after many cycles of operation. It is important to maintain a known preload to make sure the DCPS can limit upward Lorentz

load interactions with the PF coils and plasma to below the preload value. The preload mechanism has adjusting jacks that will allow recovery of the preload throughout the life of NSTX. Additionally, the preload mechanism is instrumented with two FISO displacement sensors that will allow monitoring of the preload and adjustment of the DCPS OH launching load limit, or planning a retightening of the Belleville stack adjusting jacks.

What Happens if the OH is Allowed to Operate up to 110 C? 2: More robust access to $t_{\text{discharge}} > 3\tau_{\text{CR}}$



In this configuration, only 0.2-0.4 sec of absolute discharge duration lost, despite the **fixed initial OH temperature**

Figure 4.0-21 Operation with a 110C allowable temperature limit of the OH

One conclusion of the PEER review was that the aquacement should be tested to characterize it and predict its behavior throughout the life of NSTX. It was tested in compression – see section 13.0. From the measured force deflection, the modulus is $3750 / (.0-45 / 1.25) = 104166$ psi or .0075 of copper. This means that glued to the TF, it would experience .0075 times the TF stresses, which are ~30 MPa, so the aquacement stress is tiny. It will not crack or separate.

5.0 Digital Coil Protection System.

The DCPS will be relied on to maintain the OH temperature above the TF temperature during all shots to limit frictional interaction between the TF and OH coils.

The DCPS also maintains the OH launching load below the capability of the preload mechanism to keep the OH pushed downward against the lower terminal supports and co-ax break-out. Currently the minimum compressive preload is set at 20,000 lbs in the DCPS. If the OH is allowed to operate above 100 C, creep in the OH coil will reduce this to about 15000 lbs for long

OH-TF Aquapour Interaction

NSTX
(NATIONAL SPHERICAL TORUS EXPERIMENT)
STRUCTURAL DESIGN CRITERIA
NSTX-CRIT-0001-01
February 2010

Prepared by: Irving Zatz

Concur: Peter H. Titus

Concur: _____

Approved by: _____

Digitally signed by Irving Zatz
DN: cn=Irving Zatz, o=PPPL, ou,
email=izatz@pppl.gov, c=US
Date: 2010.04.15 13:26:18 -0400

Digitally signed by Peter H. Titus
DN: cn=Peter H. Titus, ou=Research Plasma Phys,
Laboratory, cn=Engineering Admin,
email=ptitus@pppl.gov, c=US
Date: 2010.04.15 13:31:46 -0400

I. Zatz, MED Engineering

P. Titus, MED Branch Head

A. Von Halle, Head of NSTX Engineering

C. Neumeyer, NSTX Project Engineer

term operation at 110C and 10000 lbs for long term operation at 120C. The launching load limit is actually a function of OH coil energization and OH and TF temperature. To a lesser degree it is also a function of TF energization. These effects of OH coil compliance were expected to be minimal, but with the recent measured OH axial moduli, this effect needs to be included.

The loss in OH preload spring compression will scale with current squared
The increase in OH preload will scale with the thermal expansion of the OH
The decrease in OH preload will scale with the TF thermal expansion

The loss in OH preload spring compression will scale with current squared with the loss at 7mm at 24kA
The increase in OH preload will scale as: $L_{oh} \cdot \alpha_{oh} \cdot \Delta T$
The decrease in OH preload will scale with $L_{tf} \cdot \alpha_{tf} \cdot \Delta T$

6.0 Design Input

6.1 Criteria

Stress Criteria are found in the NSTX Structural Criteria Document. Disruption and thermal specifications are outlined in the GRD [7]. Stress Criteria are found in the NSTX Structural Criteria Document [1].

2.5.2.1 Mechanical Limits for Insulation Materials

The stress criteria defined herein may be locally exceeded by secondary stresses in an area whose characteristic length along the insulation plane is not more than the insulation thickness and where it can be demonstrated that cracking or surface debonding parallel to the insulation layer and limited to the local length will relieve the stresses without violating the integrity of the structure. In this situation, final verification must be obtained by mechanical/electrical testing of a representative winding pack section.

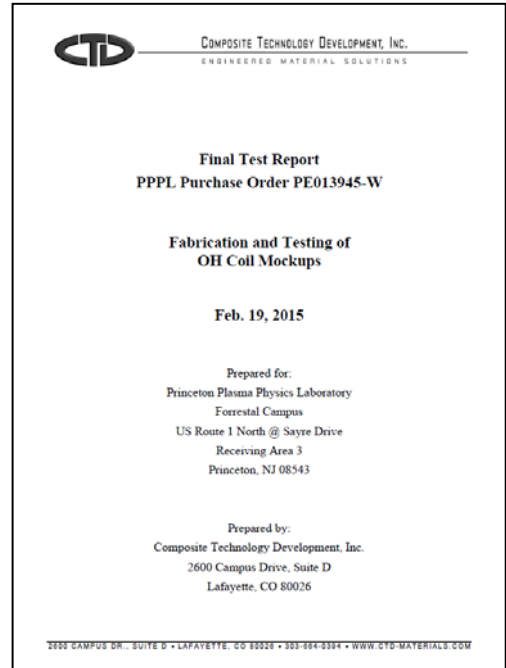
2.5.1.1.2 Tensile Strain Allowable Normal to Plane

In the direction normal to the adhesive bonds between metal and composite, no primary tensile strain is allowed. Secondary strain will be limited to 1/5 of the ultimate tensile strain. In the absence of specific data, the allowable working tensile strain is 0.02% in the insulation adjacent to the bond.

6.2 References

- [1] NSTX Structural Design Criteria Document, NSTX_DesCrit_IZ_080103.doc, Feb 2010, I. Zatz
- [2] "CALCULATION OF OH COIL STRESSES IN THE NSTX CSU" NSTXU-CALC-133-08-00, October 19, 2011 Prepared By:Ali Zolfaghari and reviewed by M. Mardenfeld
- [3] "Research Operations for NSTX-U" Stephan Gerhardt, NSTX-U Ready for Operations Review, Dec 9 2014
- [4] ITER material properties handbook, ITER document No. G 74 MA 15, file code: ITER-AK02-22401.
- [5] Time dependent scenarios transmitted by Stefan Gerhardt, and placen oGoogle Drive 8-8-2014 (These are the "Bad" Scenarios
- [6] Aquapour Supplier, Advanced Ceramics Manufacturing, 7800A S. Nogales Highway, Tucson, AZ 85756L
- [7] NSTX Upgrade General Requirements Document, NSTX_CSU-RQMTS-GRD Revision 0, C. Neumeyer, March 30, 2009
- [8] NSTX Upgrade OH Cooldown System and Preheater NSTXU-CALC-133-17-0 DRAFT December, 2014
- [9] Inner PF Coils (1a, 1b & 1c), Center Stack Upgrade NSTXU-CALC-133-01-01 March 30, 2012 Rev 0/1 by Len Myatt. Rev 2 by A Zolfaghari and A Brooks in May of 2014

- [10] "NSTXU OH Preload System and Bellville Springs"
NSTXU-CALC-133-04-00 Rev 0 October 2010, Pete Rogoff
- [11] Final Test Report, PPPL Purchase Order PE010637-W
Fabrication and Short Beam Shear Testing of Epoxy and Cyanate Ester/Glass Fiber-Copper Laminates April 8, 2011
Prepared for: Princeton Plasma Physics Laboratory Prepared by:
Composite Technology Development, Inc. 2600 Campus Drive,
Suite D Lafayette, CO 80026
- [12] Final Test Report, PPPL Purchase Order PE010925-W
Fabrication and Testing of Cyanate Ester -Epoxy /Glass Fiber/Copper Laminates, October 7 2011, Prepared for
Princeton Plasma Physics Laboratory Forrestal Campus by
Composite Technology Development Inc. 2600 Campus Drive
Suite D Lafayette CO 80026
- [13] Final Test Report, "PPPL Purchase Order PEO13945-W"
"Fabrication and Testing of OH Coil Mockups", Feb 19 2015,
Composite Technology Development Inc.
- [14] "NSTX Upgrade OH Coaxial Cable and Embedded Leads"
NSTXU-CALC-133-07-00 10 October 2011 Prepared By M.
Mardenfeld, Checked by Ali Zolfaghari
- [15] Time dependent scenarios transmitted by Stefan Gerhardt,
and placed on Google Drive 9-5 -2014 – These are the "Good"
Scenarios
- [16] OH Stress and Segmented OH Influence Coefficients for the DCPS NSTXU CALC-133-14-00 August
3 2013, P. Titus



6.3 Design Currents

6.3.1 OH and TF current Scenario

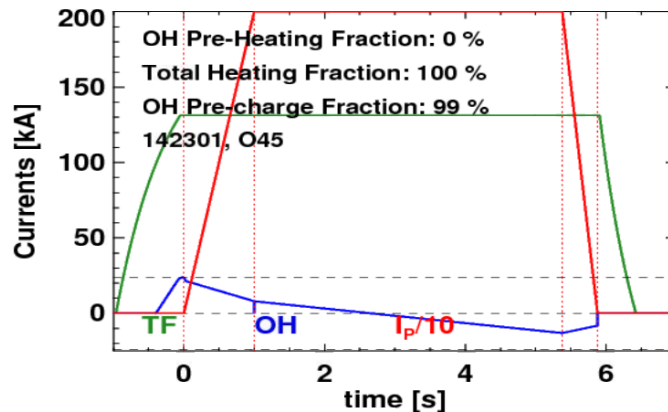


Figure 6.3-1 Coil Current Plots from the Representative Scenario

```

alpx, 5, 5e-6
ex, 17, 111e9
ex, 90, 1e6
r, 2, 1e8
r, 3, 162512/.01787/36, -.01787
mu, 2, .3
time1=0.0 $OHCur1=.0001 $OHtemp1=12 $TFCur1=0 $TFTemp1=12
time2=0.5 $OHCur2=.0001 $OHtemp2=12 $TFCur2=0 $TFTemp2=12
time3=1.0 $OHCur3=24 $OHtemp3=20 $TFCur3=0 $TFTemp3=18.38
time4=1.5 $OHCur4=17 $OHtemp4=35 $TFCur4=130 $TFTemp4=24.7
time5=2.0 $OHCur5=10 $OHtemp5=47 $TFCur5=130 $TFTemp5=31.1
time6=2.5 $OHCur6=7 $OHtemp6=50 $TFCur6=130 $TFTemp6=37.5
time7=3.0 $OHCur7=3 $OHtemp7=50 $TFCur7=130 $TFTemp7=43.9

```

```

time8=3.5   $OHCur8=1   $OHtemp8=50   $TFCur8=130   $TFTemp8=50.3
time9=4.0   $OHCur9=.0001   $OHtemp9=50   $TFCur9=130   $TFTemp9=56.7
time10=4.5  $OHCur10=-1   $OHtemp10=50   $TFCur10=130   $TFTemp10=63.07
time11=5.0  $OHCur11=-3   $OHtemp11=50   $TFCur11=130   $TFTemp11=69.46
time12=5.5  $OHCur12=-6   $OHtemp12=52.5 $TFCur12=130   $TFTemp12=75.8
time13=6.0  $OHCur13=-9   $OHtemp13=55   $TFCur13=130   $TFTemp13=82.25
time14=6.5  $OHCur14=-12  $OHtemp14=57.5 $TFCur14=130   $TFTemp14=88.6
time15=7.0  $OHCur15=-10  $OHtemp15=60   $TFCur15=130   $TFTemp15=95
time16=7.5  $OHCur16=.0001 $OHtemp16=60   $TFCur16=0     $TFTemp16=12

```

6.3.2 “Bad Scenarios”

Scenarios from Stefan Gerhard representing “bad” scenarios in that they deliberately aggravate the interaction between the OH and TF are included in reference 5, transmittal email listed in Appendix A.

6.3.3 “Good Scenarios”

Scenarios from Stefan Gerhard representing “good” scenarios in that they avoid or minimize the interaction between the OH and TF are included in reference 15, transmittal email listed in Appendix A.

6.4 Materials and Allowables

The important material properties and allowables are those of the insulation. First, the tensile bond strength was measured for the TF. It is cyclically dependent and is about 14 MPa for the life required of NSTX-U. A reasonable design limit would be half this. For the OH winding pack, the allowable is substantially diminished by the inclusion of Kapton.

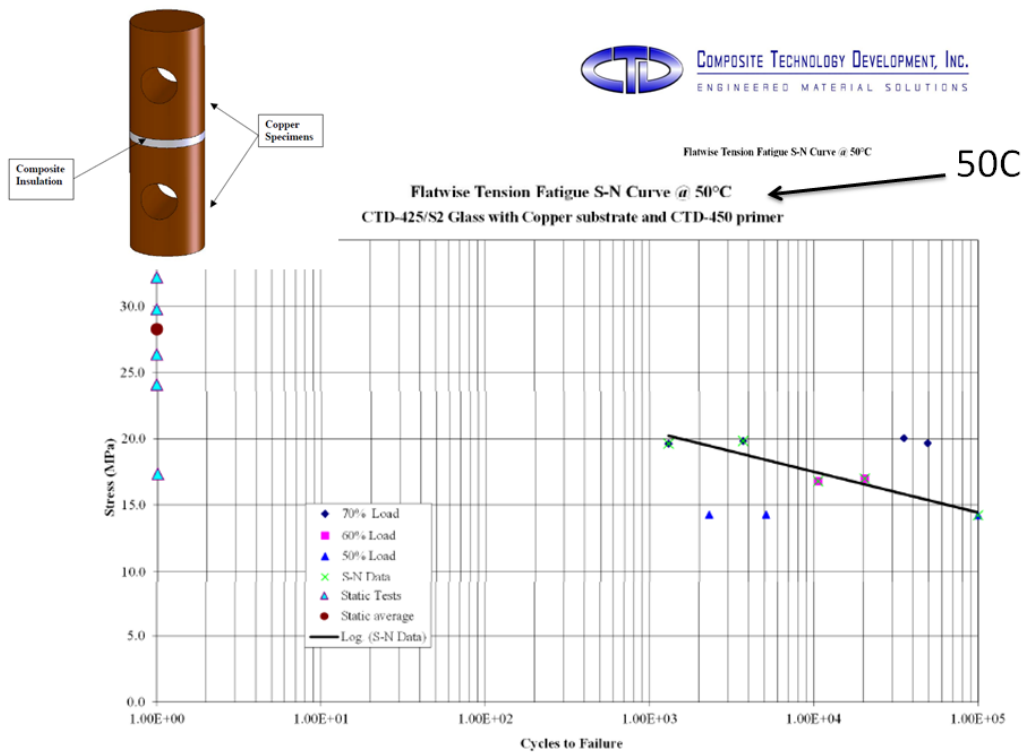
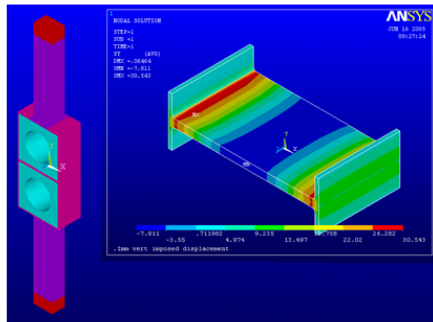


Figure 6.4-1 Fatigue Tensile Strength of the CTD 425 Syster (Without Kapton)



PSFC-RR-06-1
Desktop Vacuum Pressure Impregnation Experiment for ITER Insulation Testing
 Mahar S., Titus P., Gung C., Hooker M., Mierovini J., Schultz J., Stable P., Takayasu M.
 April 2006

- Broke at only 100 lbs
- Broke at Kapton Bonds
- Withstood 21kV after air gap tracking fixed.

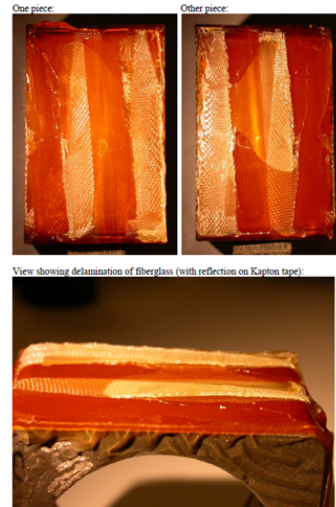


Figure 6.4-2 MIT tests of Insulation with Interleaved Kapton/glass

Small tests done at MIT showed almost no tensile strength when Kapton was added. The insulation system, however, was capable of withstanding 21 kV after the sample was reassembled and flash shields added. More extensive measurements of the tensile strain allowable is discussed in section 14.0.

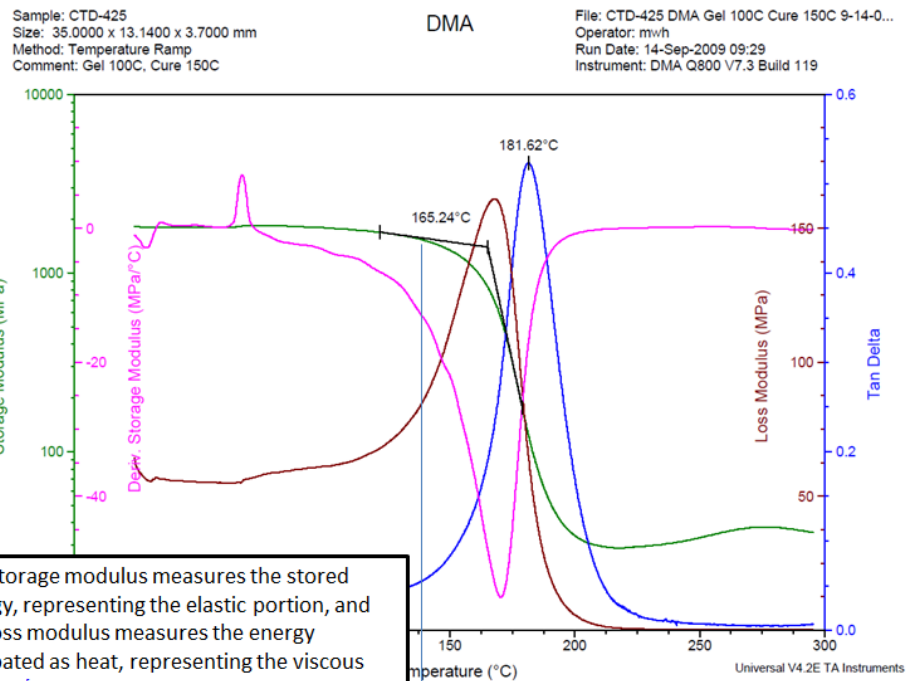


Figure 6.4-3 CTD-425 storage modulus Plot

The transition from elastic to plastic is the glass transition temperature. This is about 170 degrees C or about the cure temperature. More extensive measurements of the tensile strain allowable is discussed in section 14.0.

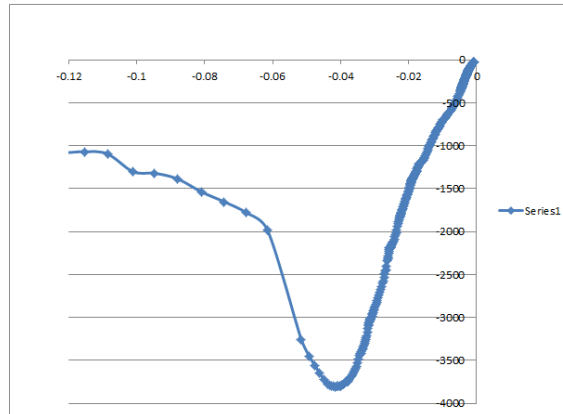


Figure 6.4-4 Measured "Aquacement" Force Deflection

7.0 Models

7.1 Heat-Up Test Models

A water soluble material called Aquapour [6] was intended to create a gap between the TF and the Ohmic Heating (OH) coil, which was wound onto the TF coil. The VPI penetrated the AQUAPOUR and it could not be removed. When the coil assembly was still on the winding machine, the OH was heated above the TF temperature to see if it would slip. It did, which indicated that at least the parting plane between the two coils was established. It is assumed that the slip plane measured during heating tests is at the Teflon sheet surrounding the Aquapour. The analysis results using this model are included in Section 8.0.

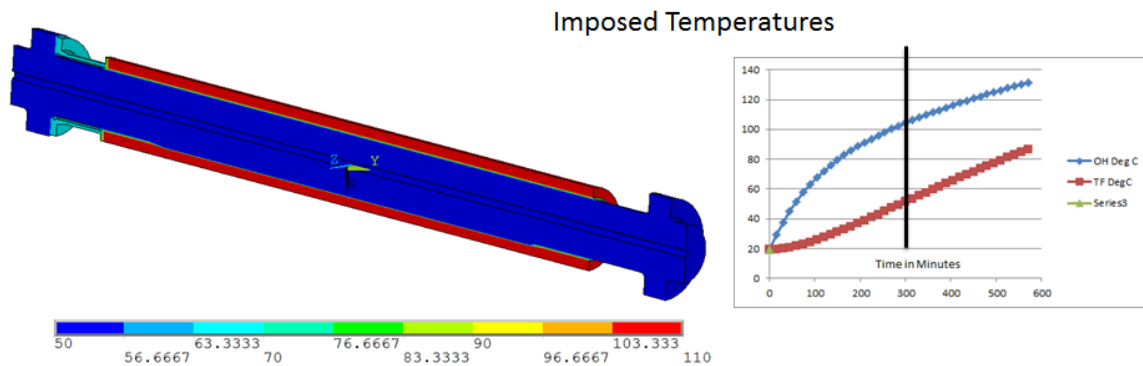


Figure 7.1-1 Model Used for the Heat-Up Tests in the Winding Area

The Aquapour interface was modeled with interface 52 node-to-node gap elements. A 3D model is used for many of the studies, even though the problem is basically 2D. The model was first developed to investigate the interaction between the OH and TF in the winding area when the centerstack windings were still on the winding machine. The interface 52 gap elements were used because they have a faster solution time, and the mesh was aligned across the interface between the two coils.

7.2 Models Used to Simulate Frictional Interaction during Operation

The model used for the heating simulations on the winding machine was improved to simulate the frictional interaction of the TF and OH coils during

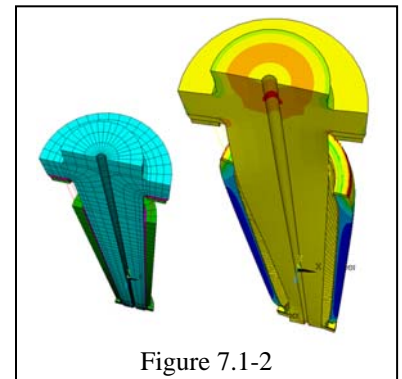


Figure 7.1-2

operation. The preload mechanism had to be added to the model as this was not in place (or at least was not preloaded when the heating tests were performed). The preload mechanism was modeled using the Gap 52 elements with stiffnesses calculated from the Belleville stack stiffness from [10]. A portion of the loads table from [10] is shown below. The total gap stiffness (summed over all the gaps at the interface) is set at 162512/.01787 N/m.

System scenario	Compression mm	Force on OH N	Force on OH lbs.*	Tensile Stress N/mm	Fatigue Cycles
Pre Load	17.87	162,512	36,520.	849.	-----

Figure 7.2-1 Excerpt from the Table in [10]

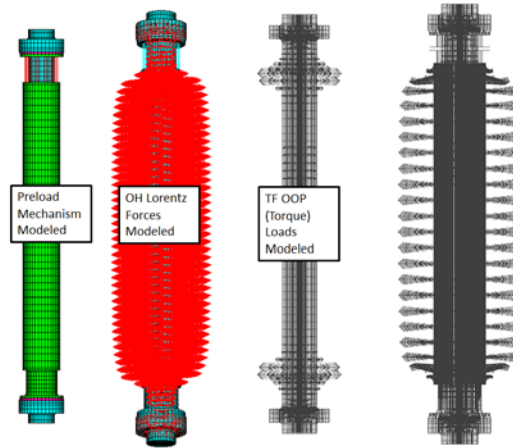


Figure 7.2-2 Aquapour Friction Interaction Model

During operation, Lorentz forces have the potential to radially expand the OH coil and reduce the frictional load at the OH-TF interface. The Lorentz loads were computed and stored in a load file that could be scaled by the square of the OH current in the scenario being studied.

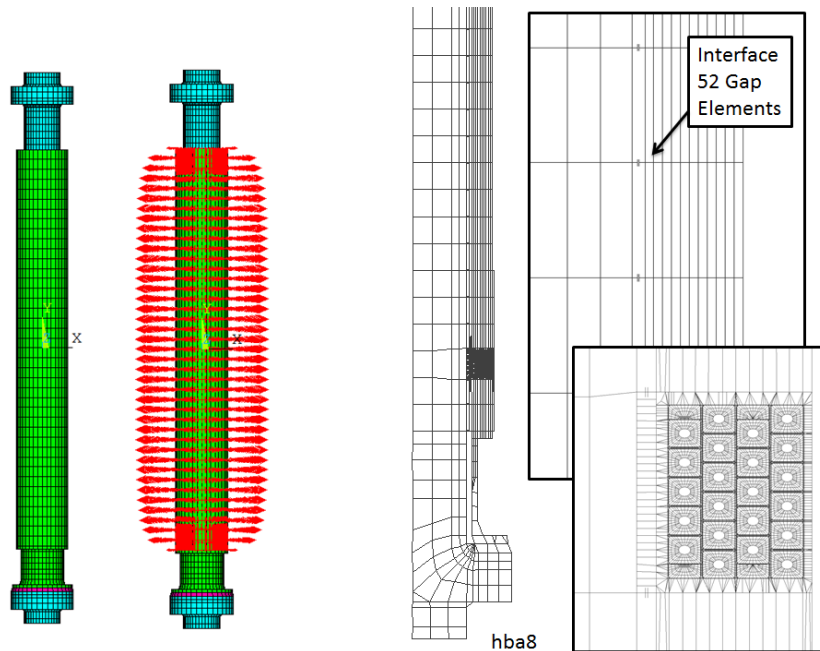


Figure 7.2-3 "Hybrid" Aquapour Friction Interaction Model with Smeared OH properties and a section with a discrete modeling of the conductors

7.3 Smeared OH Properties

The axial modulus is an important parameter in analyses intending to quantify the axial stress or strain in the OH coil. For the simulation of heating the OH on the winding machine, the axial loads that would overcome bonding and friction between the two coils is a function of how compliant the coil is. The axial modulus is also important in understanding the loads that would overcome frictional interactions between the OH and TF coils. The hoop direction is dominated by the copper percentage. Radial and vertical directions are dominated by the compliance of the Kapton/glass insulations system.

From reference [8] section 7.1.1, the winding pack radial and vertical composite moduli were computed to be ~85 MPa. This was calculated from the percentages of copper and insulator or from winding pack finite element models. The axial winding pack modulus was also measured in two different tests done by CTD. The tensile modulus is measured in tests discussed in Section 14, and in Figure 14.0-5 can be seen to range from 3.2 down to 1 GPa late in its cyclic life. Compressive moduli have been estimated from both creep compression tests by CTD and measured displacements of the OH coil during the April 2015 NSTX-U run. The compressive modulus is estimated to be between 20 and 30 GPa.

8.0 Simulation of Heat-Up Tests

8.1 August 1, 2014 Presentation, July 2014 Tests

Current was run through the OH when it and the TF were mounted horizontally on the winding machine in accordance with NSTX Procedure # D-NSTX-RP-CL-001.

A transient thermal simulation was performed using a spreadsheet analysis that included Joule heat of the OH, convective losses to the air around the coils, conduction through the Aquapour to the TF and later, cooling of the TF. The intention was to break the OH and Aquapour free of the TF and possibly facilitate removal of the Aquapour.

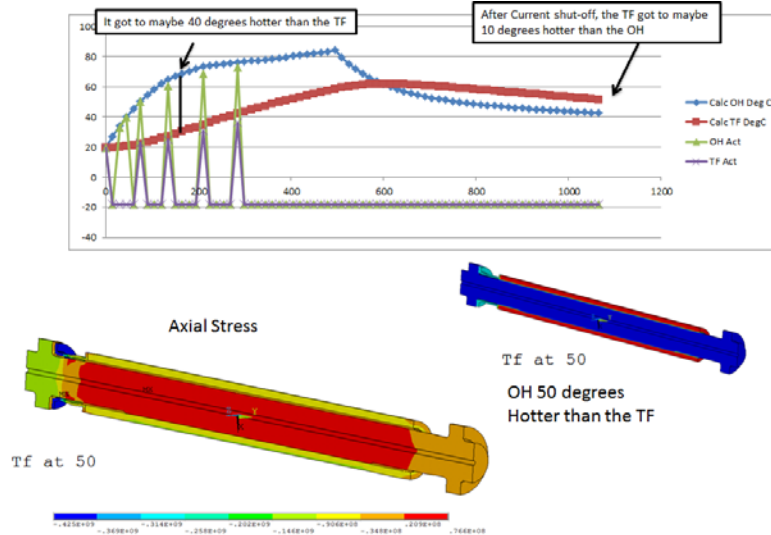


Figure 8.1-1 Simulation of the OH Heating Intended to Break up the Aquapour.

The simulation tracked the measured temperatures of the OH pretty well and showed that there was significant leakage of heat from the OH to the TF limiting the differential temperatures between the two coils.

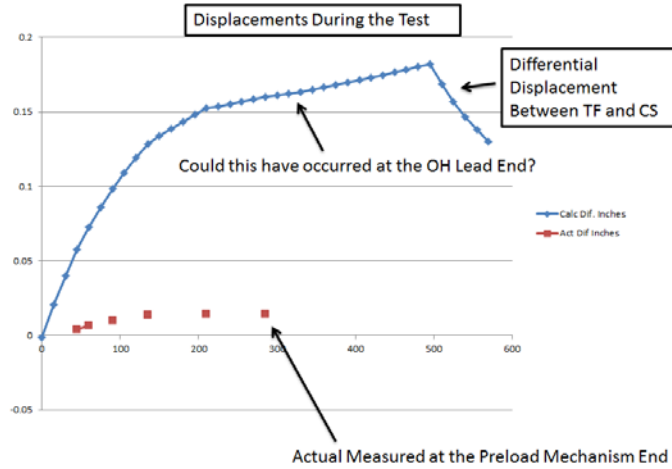


Figure 8.1-2 Displacements from the Simulation and Measured Values.

In Figure 8.1-2 the displacements at the preload mechanism end are plotted for both the calculated and measured values. The difference was a mystery until it was noted by Steve Raftopoulos that there was an initial gap at the terminal end that closed during the heating. The gap was approximately the size of the missing displacement. So the coil expanded away from the preload mechanism end and the gap closed. And the dial indicator measured very little of the total displacement. As the OH coil is heated, it loses heat to the TF and then the differential temperature is less. If the TF is actively cooled from the beginning, the current in the OH is not large enough to overcome the TF heat leak and the OH does not get as hot. It was suggested that the TF not be cooled for 180 seconds and then turn on the TF cooling. This would quickly lower the temperature in the TF and increase the differential temperature and hopefully break up the Aquapour. This approach yielded the bigger differential temperature, but unfortunately did not break up any Aquapour.

Suggestion for the Next Test – TF Provide Cooling after about 180 minutes
Then maintain it until the OH is at RT

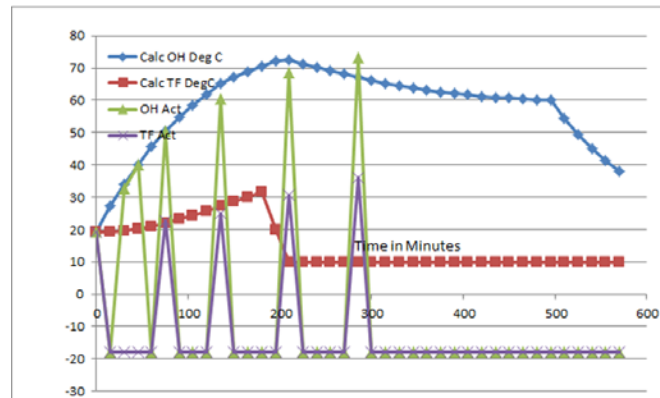


Figure 8.1-3 Heating profile with a later addition of TF cooling

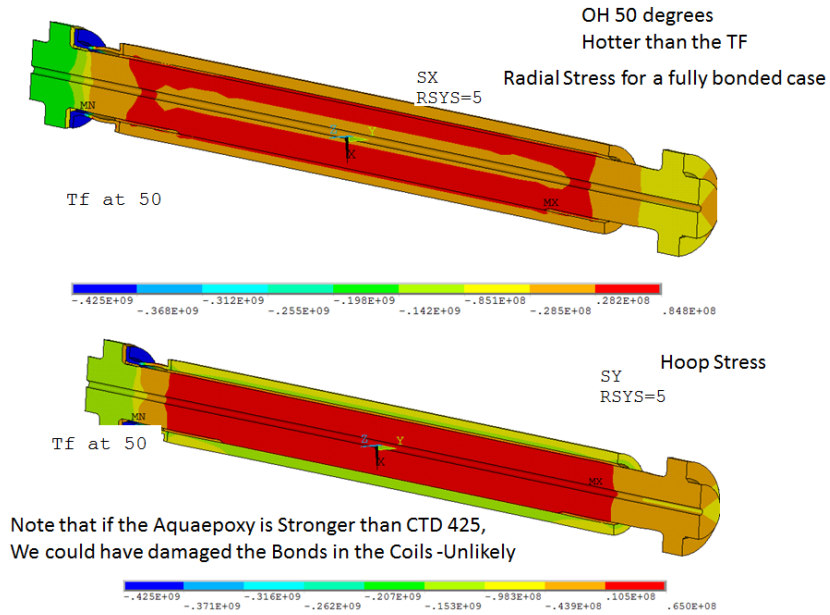


Figure 8.1-4 OH Coil 50C Hotter than the TF

In figure 8.1-4 the interface between the OH and TF is fully bonded. It is unlikely that the aquapour could have sustained the radial stress that would have developed, especially because of the Teflon parting plane that is between the coils.

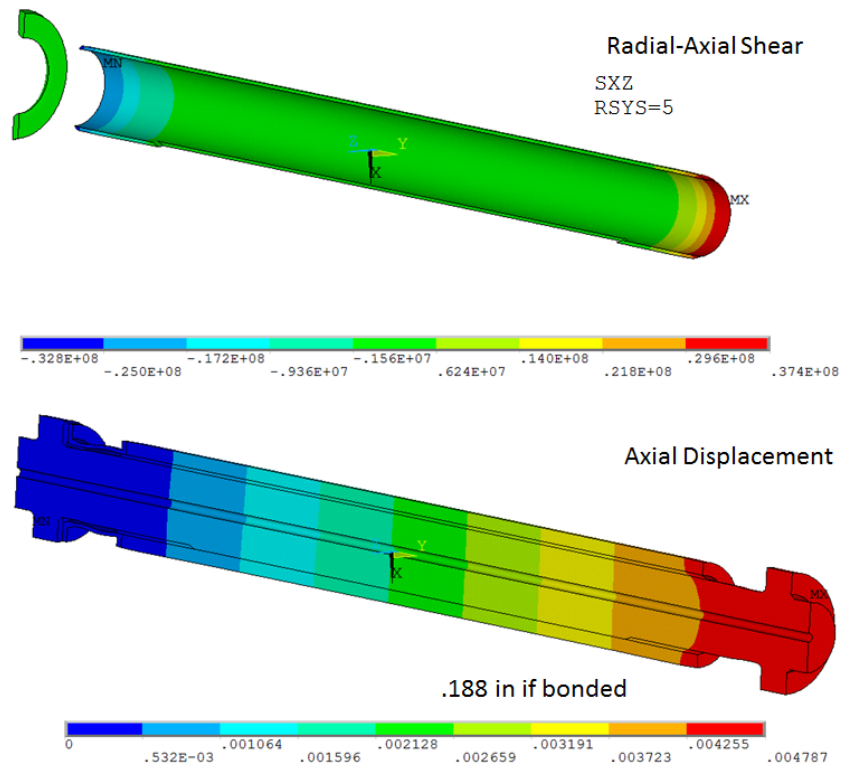


Figure 8.1-5 Radial and Axial Shear and Axial Displacement if bonded.

The radial axial shear would be 37 MPa if the aquapour was fully stuck to both the OH and to the TF. The growth of the two coils stuck together would be 4.787mm or .188 inches.

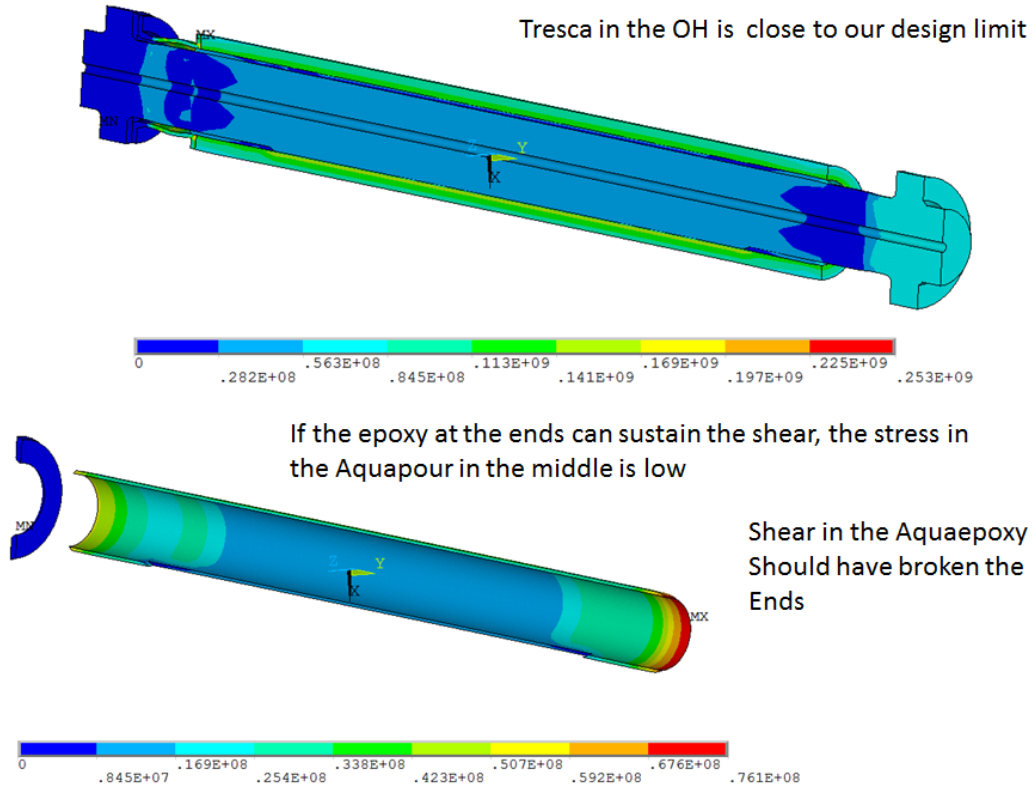


Figure 8.1-6 OH Coil Tresca and Radial-Axial Shear

The shear-lag stress at the ends of the aquapour, shown in figure 8.1-6 should have broken the coil free. This proved to be what happened. The dial indicators were at the preload mechanism end. However a gap was observed at the other end by Steve Raftopoulos This closed when the OH cooled.

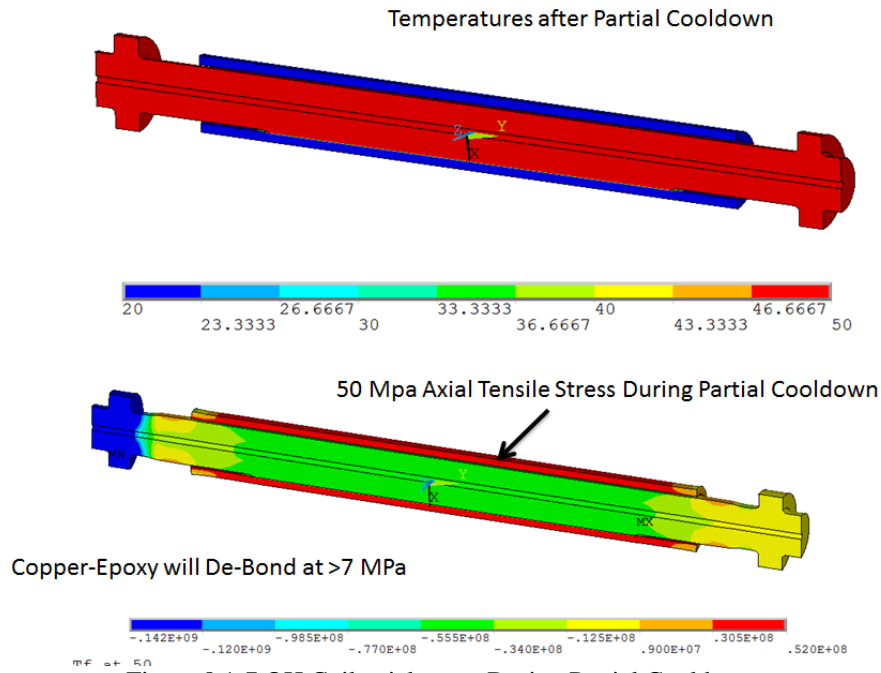


Figure 8.1-7 OH Coil axial stress During Partial Cooldown,

The stress result shown in figure 8.1-7 was intended to be a cautionary analysis to show what would happen if the OH was allowed to cool faster than the TF. The OH would lose heat by convection faster than the TF. This effect was shown in the simulation shown in figure 8.1-1. Cooling water was added to the TF for this reason, but mainly to improve the differential temperature between the coils. The effect of cooling was shown in figure 8.1-3

9.0 Simulation of Frictional Interaction with OH Lorentz Loads, Only, Smeared OH Properties

S.Gerhardt provided an early example of an OH/TF scenario to assess the interaction between coils. Data for this scenario is included in section 6.3. Only OH and TF currents were provided. Later full PF scenarios were evaluated by Han Zhang (section 11.2). It is conceivable that the extra OH hoop tension due to interactions with PF1a might affect the OH/TF interactions. It is unlikely that the other PF coils can effect OH hoop stress enough to change the radial pressure between OH and TF. The model discussed in section 7.2 was used to investigate the behavior of this “scenario”. The stress at the base of the OH coil was omitted from the Aquapour interaction study because lower end of the OH coil has had special consideration in other calculations [2] [8] [14] in which local details of the interaction with the stepped G-10 support shell and Co-ax Box are more significant than effects of the Aquapour interaction. For this study, the tension stresses at about ½ meter from the bottom of the OH coil are tabulated for various TF and OH temperatures and various friction coefficients. If TF/OH frictional interactions are allowed, stresses at the OH base may need to be re-considered.

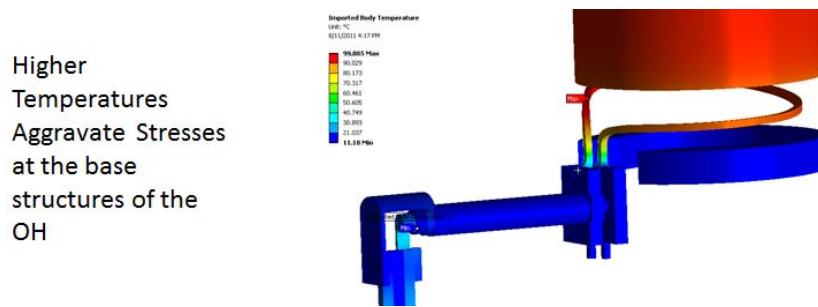


Figure 9.0-1, Excerpt from [14] Showing Details of the OH Base that were Modeled

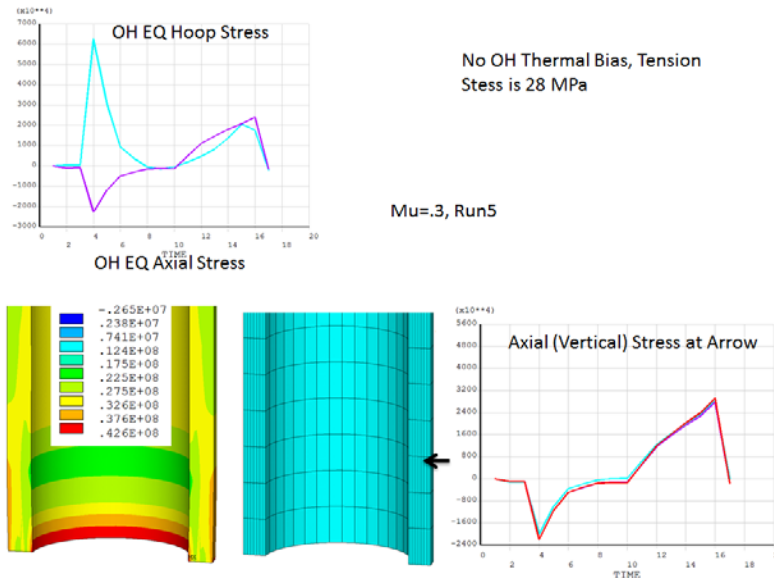


Figure 9.0-2 Initial Results for OH Hoop and Axial Stress for an initial OH/TF Current Scenario

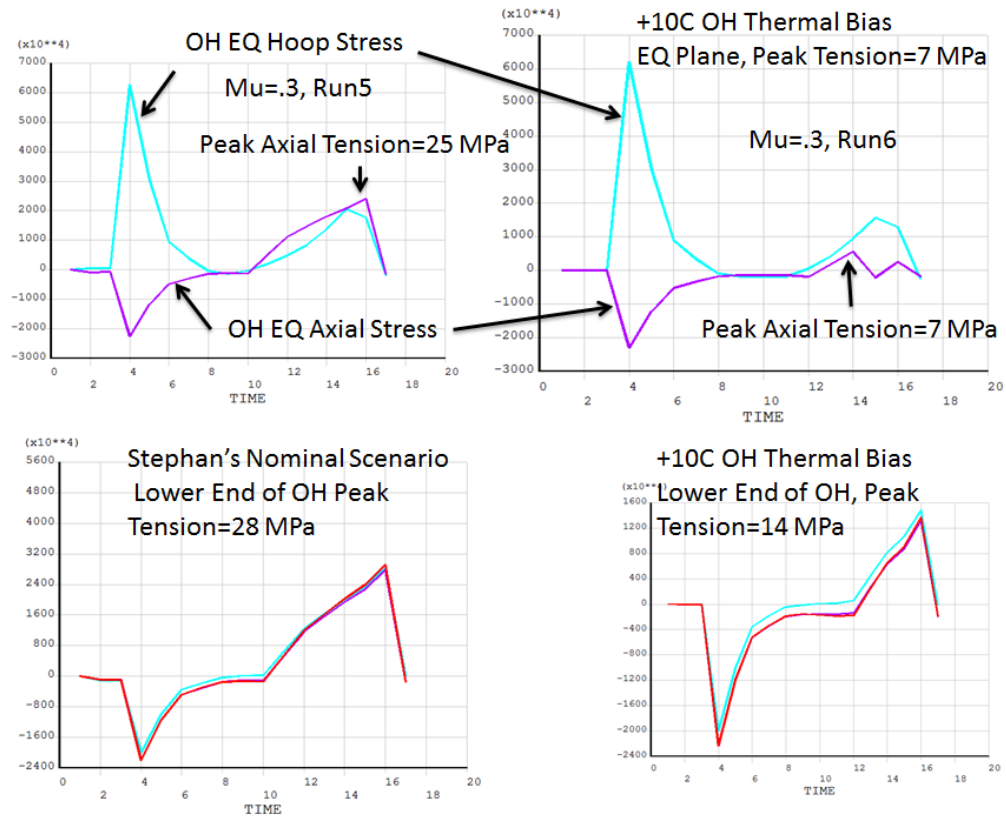


Figure 9.0-3 OH Hoop and Axial Stress with 10C OH bias for an initial OH/TF Current Scenario

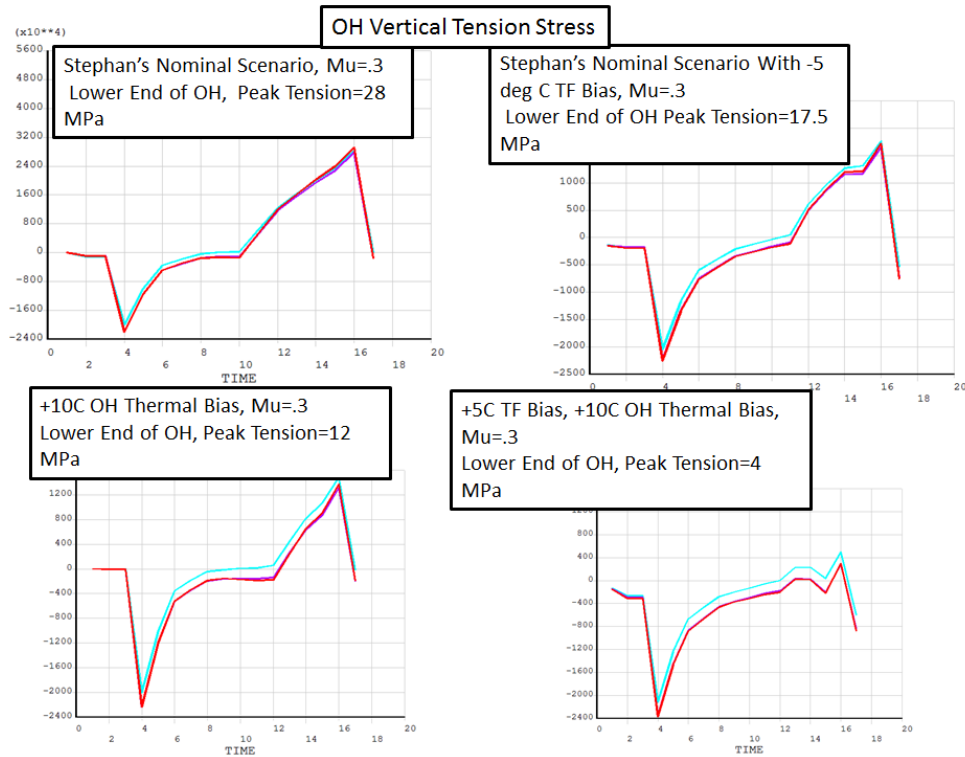


Figure 9.0-4 OH Axial Stress with 10C OH and TF bias for an initial OH/TF Current Scenario

9.1 Effect of Preload Mechanism to Offset the Tensile Stress

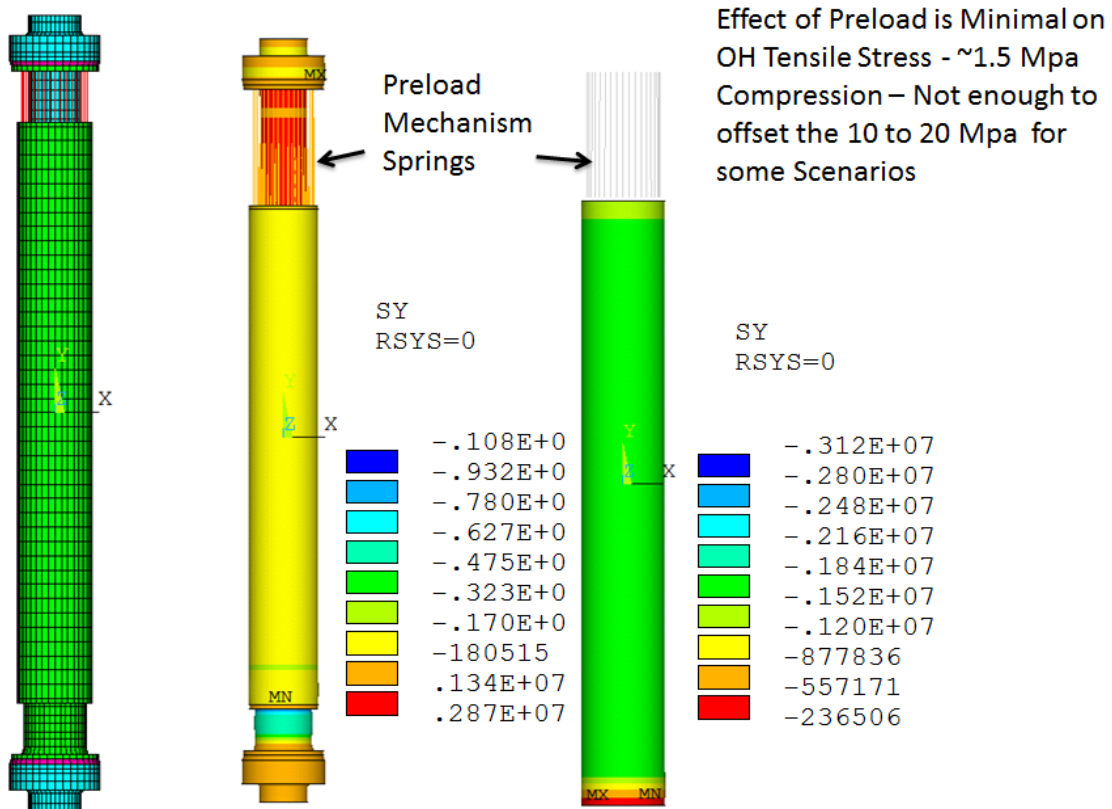


Figure 9.1-1 OH/TF model with the preload applied and no Lorentz Loads and no thermal differentials

In this calculation, just the preload mechanism nominal load was applied. From [10] the nominal preload for 17.87mm compression in the Belleville stacks is 36520 lbs or 162512 Newtons (a table from this calculation is also included in Figure 15.1-5). The cross section of the OH is $\text{Pi} \cdot (.2768^2 - .2074^2) = .105568 \text{ m}^2$ and the nominal axial compressive stress is $162512 / .105568 = 1.53 \text{ MPa}$. This simply confirms that the gap elements that model the preload mechanism are input correctly.

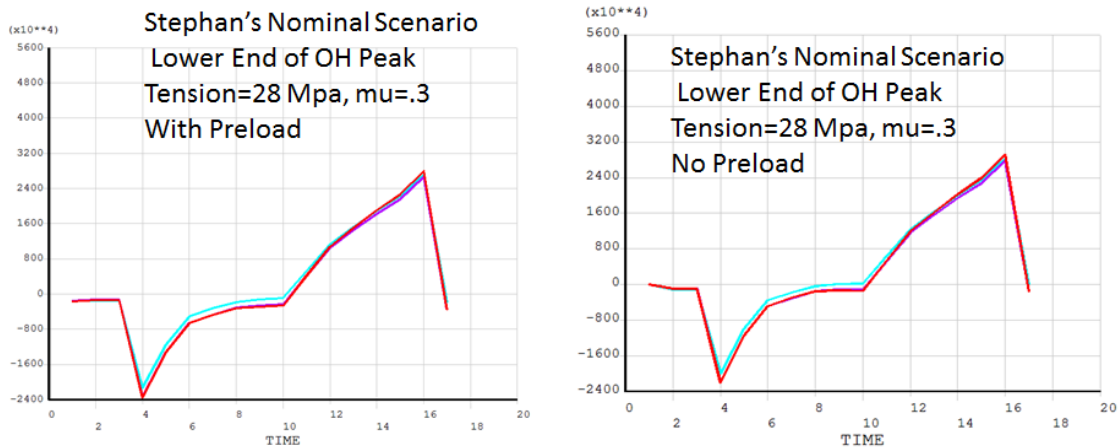
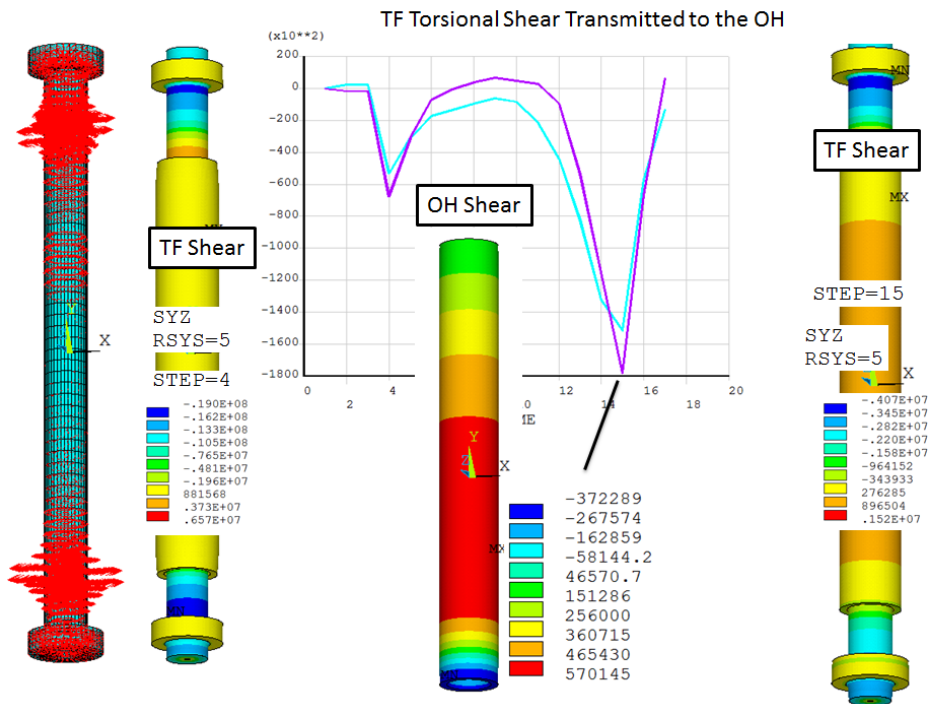
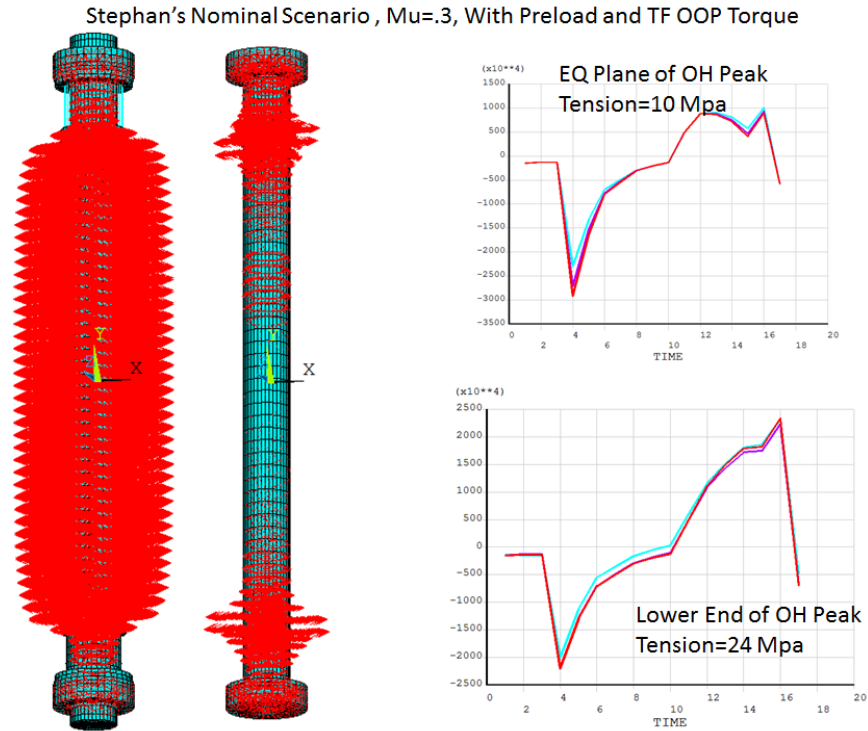


Figure 9.1-2 No Difference results for Runs With and Without Preload

9.2 Torsional Shear Stress in the OH if it is Frictionally Connected to the TF



10.0 Simulation of 14 (Bad) Equilibria Supplied by Stefan Gerhardt (by Han Zhang)

On August 8, 2014 S. Gerhardt provided 14 “bad” Scenarios [5] intended to quantify a simple rule of thumb relating the OH axial tension to the difference in temperature between the TF and OH. These scenarios produced a range of TF temperatures that were greater than the OH temperature throughout the pulse. As before, path dependent simulations were performed and the temperature difference and OH axial stress noted. In these analyses, Zhang used the OH load file d=for 24 kA terminal current provided by P. Titus.

The TF/OH model with the frictional interface was run with friction coefficients of .1 and .3. The peak tensile stress at the bottom of the OH and the tensile stress about ½ meter from the bottom are tabulated at right. For this study, No Lorentz forces are included in either the TF or OH. The OH temperature is held constant, and then TF temperature increase is ramped.

Stefan Provided Han with 14 Scenarios with different OH biases and TF-OH temperature differentials. OH tensile stress about ½ meter from the bottom is tabulated at right. For this study, OH Lorentz forces are included.

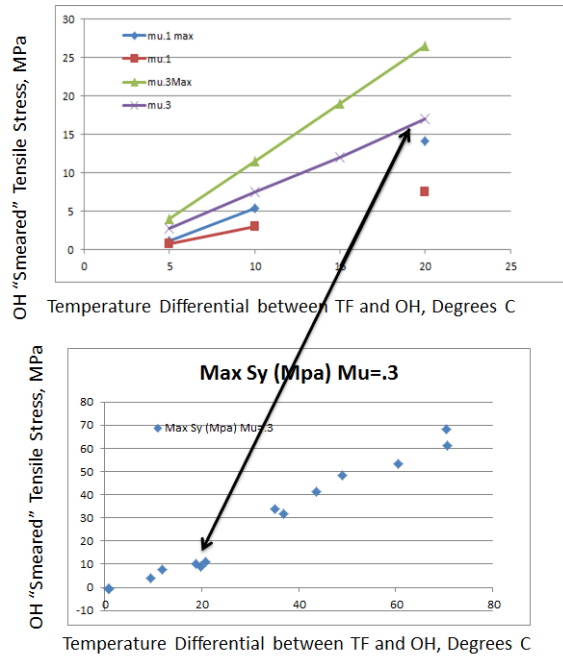


Figure 10.0-1 Comparison of Titus without OH Lorentz (Upper) and Han Zhang with OH Lorentz (Lower) Sy vs Delta T

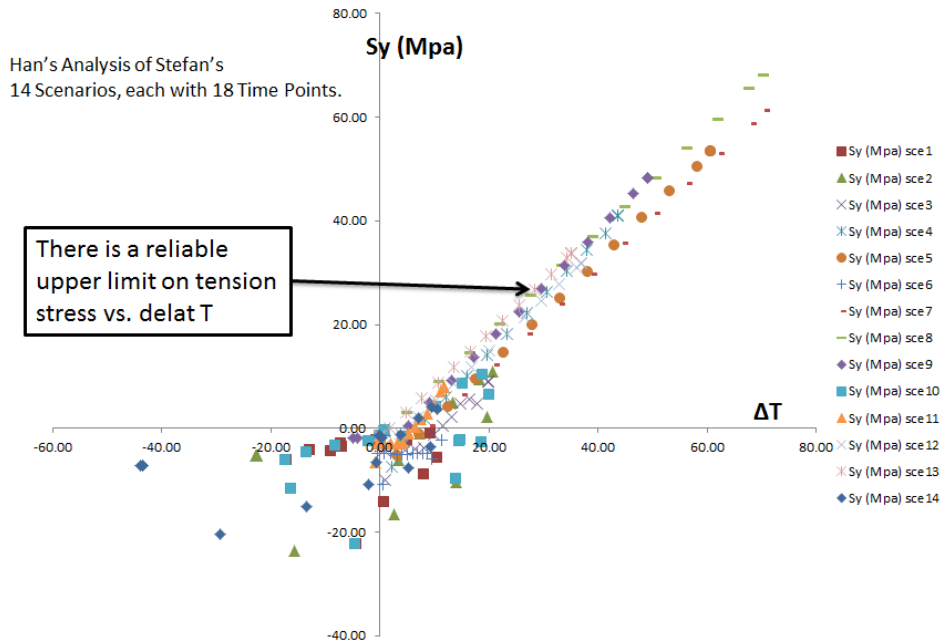


Figure 10.0-2 OH Axial Stress vs TF-OH Temperature Difference – All Points

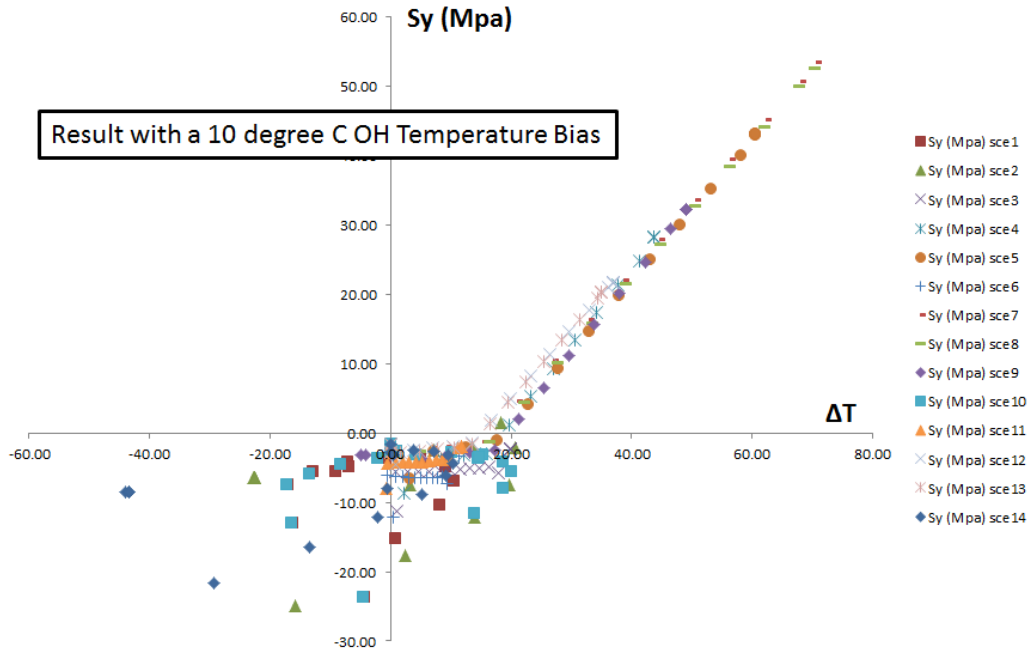


Figure 10.0-3 OH Axial Stress vs TF-OH Temperature Difference, With 10C Bias – All Points

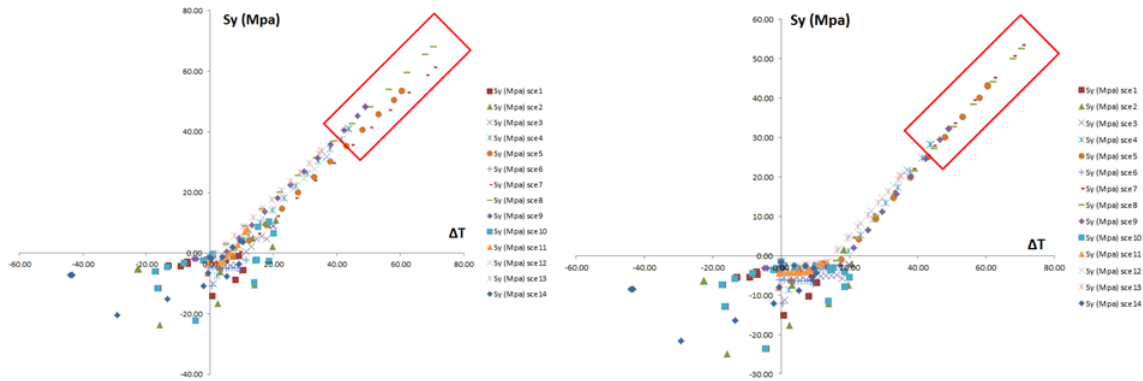
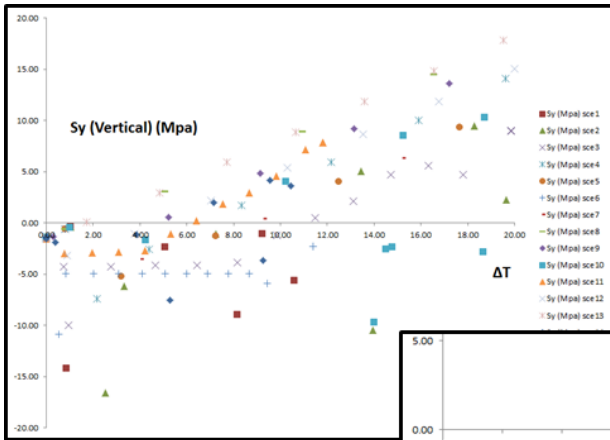


Figure 10.0-4 OH Axial Stress vs TF-OH Temperature Difference, With and Without 10C Bias – All Points

In a Sept 8th 2014 email, H. Zhang pointed out that there was an interesting behavior. In the Sy_delta T plots shown in figure 10.0-4, one without temp bias and the other with 10 degree C temp bias in OH coil, there is possibly a stick slip behavior in which the OH “locked in” a small amount of compression probably from the pre-charge that later subtracted from the TF expansion effect. When the bias was added, the OH probably did not “stick” at the pre-charge and was “grabbed” by the TF later when there was no compression in the OH. This is an indication of the path dependent behavior of the interaction.

11.0 Simulation of 14 (Good) Equilibria Supplied by Stefan Gerhardt (by Han Zhang)

On Sept 5, 2014, Stefan Gerhardt provided a set of “good” scenarios [15] in which the interaction between the OH and TF was eliminated or mitigated. The scenarios kept the TF no more than 10 degrees C above the OH. These scenarios were also run with a 10 degree bias which eliminated the axial tension in the OH coil.



Relationship is more complex in the delta T regime in which we expect to operate.

But still, keeping the delta T below 10C keeps the stress below 10 MPa

With a 10C OH Bias, All the stresses are compressive up to ~16 degrees C

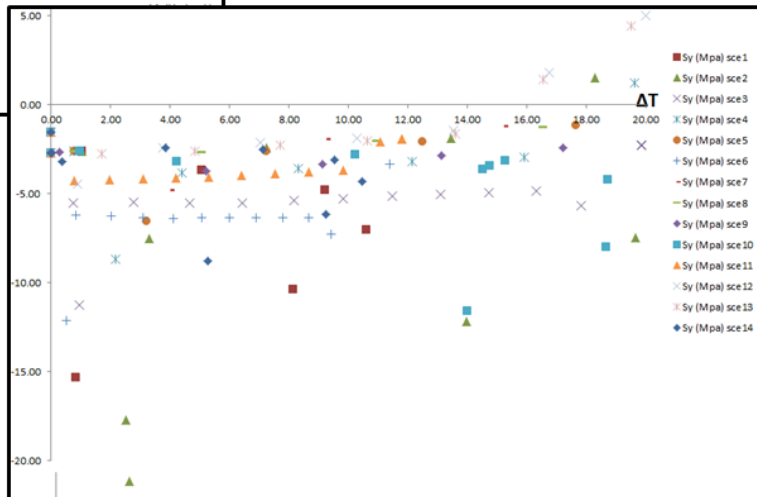
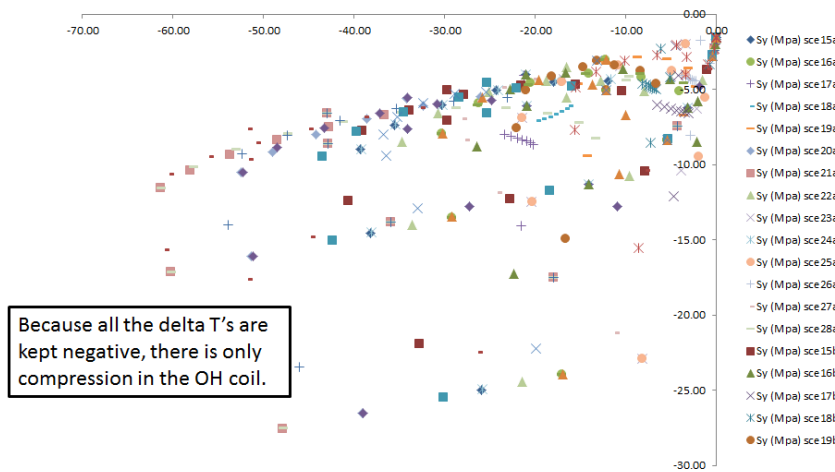


Figure 11.0-1 OH axial tension as a function of delta T

11.1 Simulation of 14 Equilibria with Full OH Loading

In a Sept 6th 2014 transmittal, S. Gerhardt added a few more 2 MA scenarios, varying from rather high to rather pathetic levels of confinement. Again, the pre-heat and recharge adjusted to always keep $T_{TF} < T_{OH}$ and allowing 110 C operations. Gerhardt suggested focusing on these + Pete19 and Pete20. These are all the 2 MA cases.



Because all the delta T's are kept negative, there is only compression in the OH coil.

The new files all keep $T_{TF} < T_{OH}$, sometimes with a large margin and sometimes not. The cases with 2 MA (15a,15b,16a,16b) do use the 110 C option, though most of the others don't. Anyway, the 15a and 15b cases have the same current and loop voltage, but different pre-heat, pre-charge. And the 16a and 16b cases are the same current and loop voltage (but different than 15), but different pre-heat and pre-charge. And so on, where the "a","b","c" indicated essentially different ways that we might run the plasma current value.

Figure 11.1-1 OH axial stress vs TF-OH temperature

Because all the delta-T stayed negative, there is only compression in the OH coil.

11.2 Simulation of 14 Equilibria with Full PF Loading

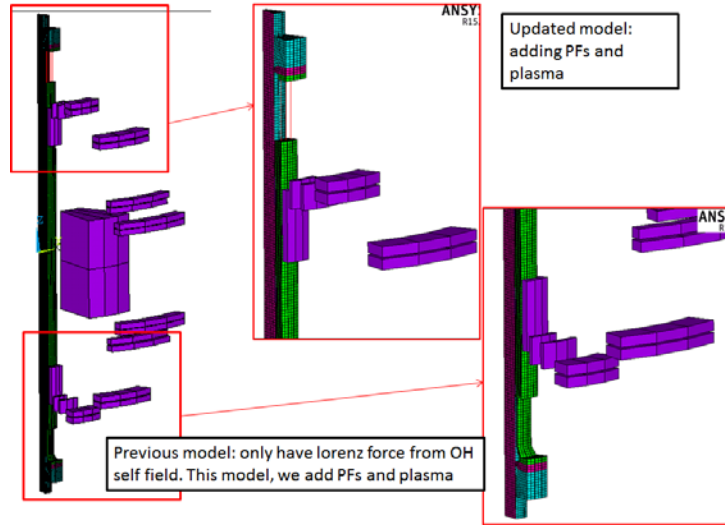


Figure 11.2-1 Model with PF Coils and Plasma Added.

Interactions with the inner PF coils can add hoop tension stress to the OH. This was found to limit the pre-charge currents allowed in the OH if PF1a is used along with the OH. This is the subject of a special DCPS algorithm in [16] NSTXU-CALC-133-14-00. The extra hoop stress can change the way the coil interacts with the TF through the aquapour.

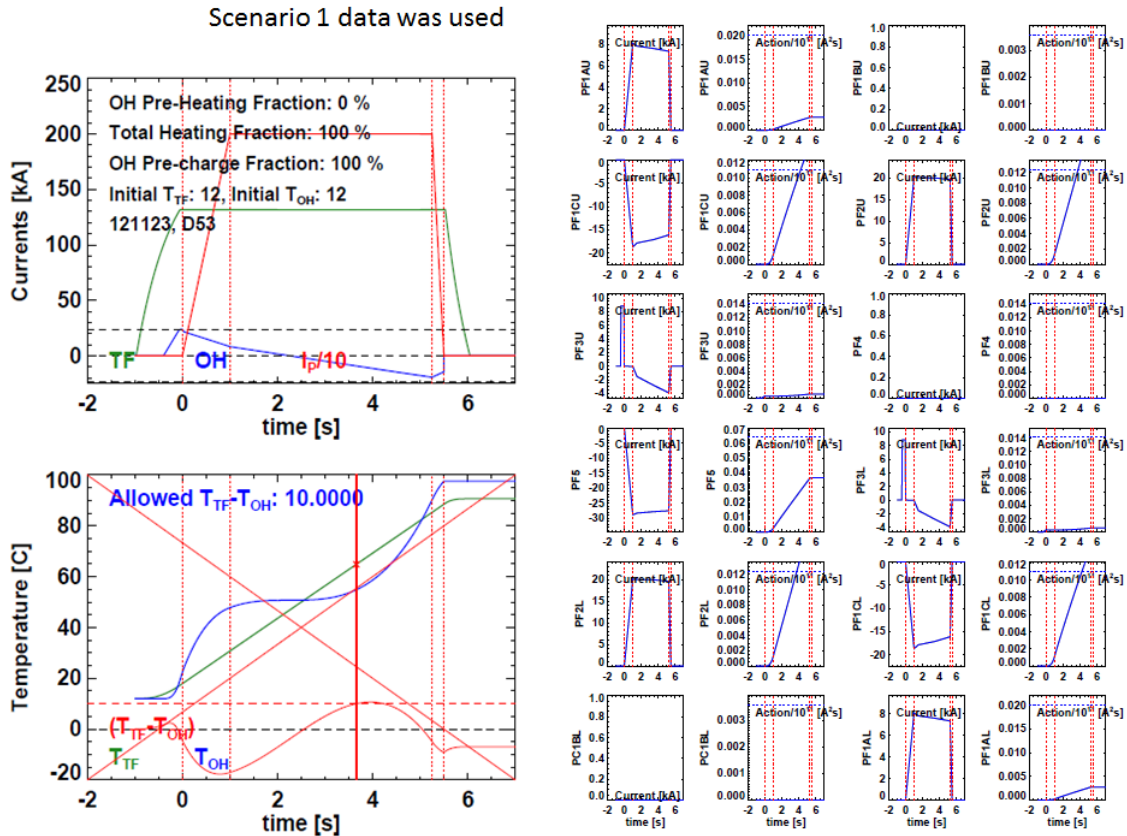


Figure 11.2-2 Scenario 1 Data from Stefan Gerhardt.

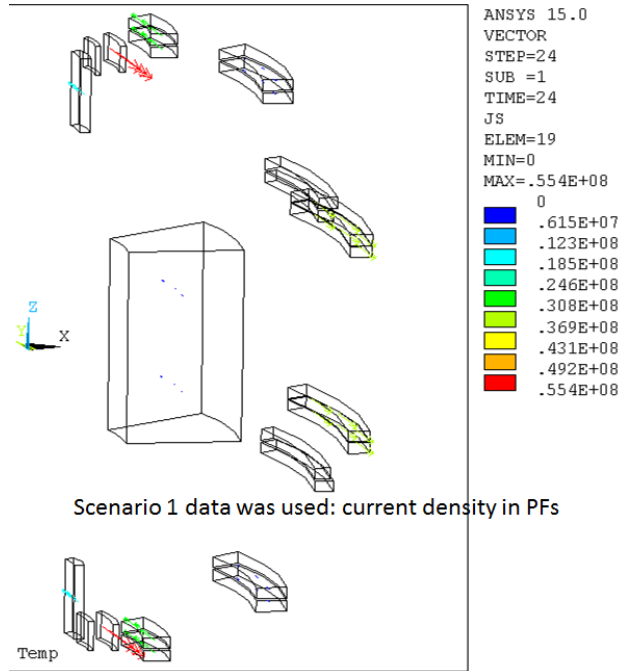


Figure 11.2-3 PF Current Densities.

Scenario 1 data was used: current density

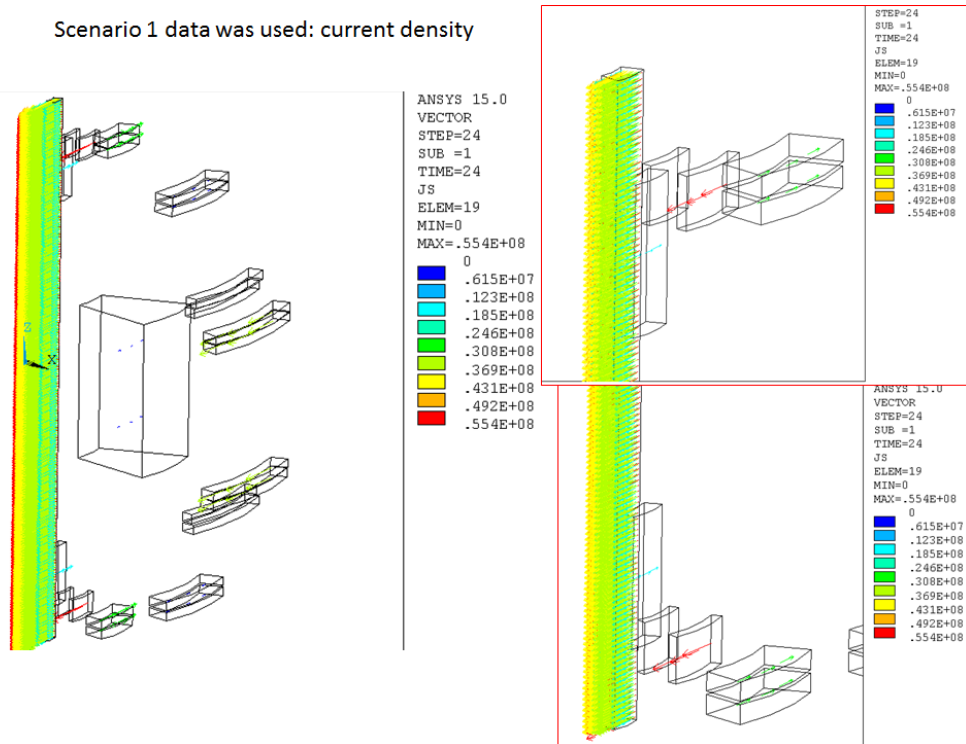


Figure 11.2-4 PF Current Densities – Including OH

Scenario 1 data was used: current density

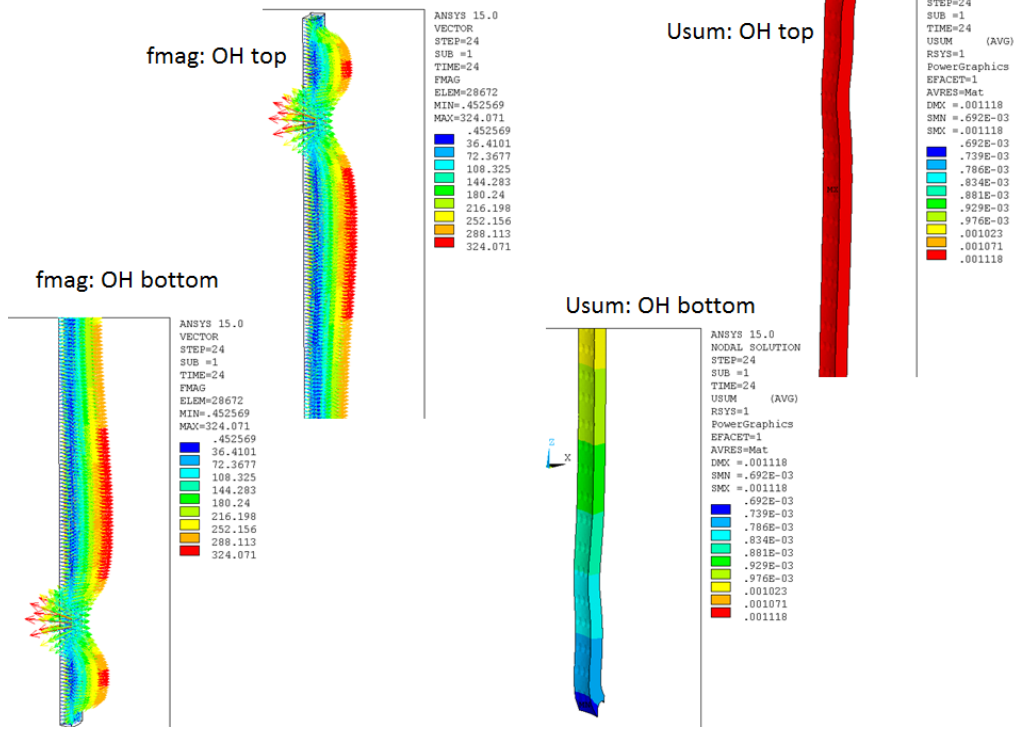


Figure 11.2-5 OH Forces and Displacements

Scenario 1 data was used: displacement

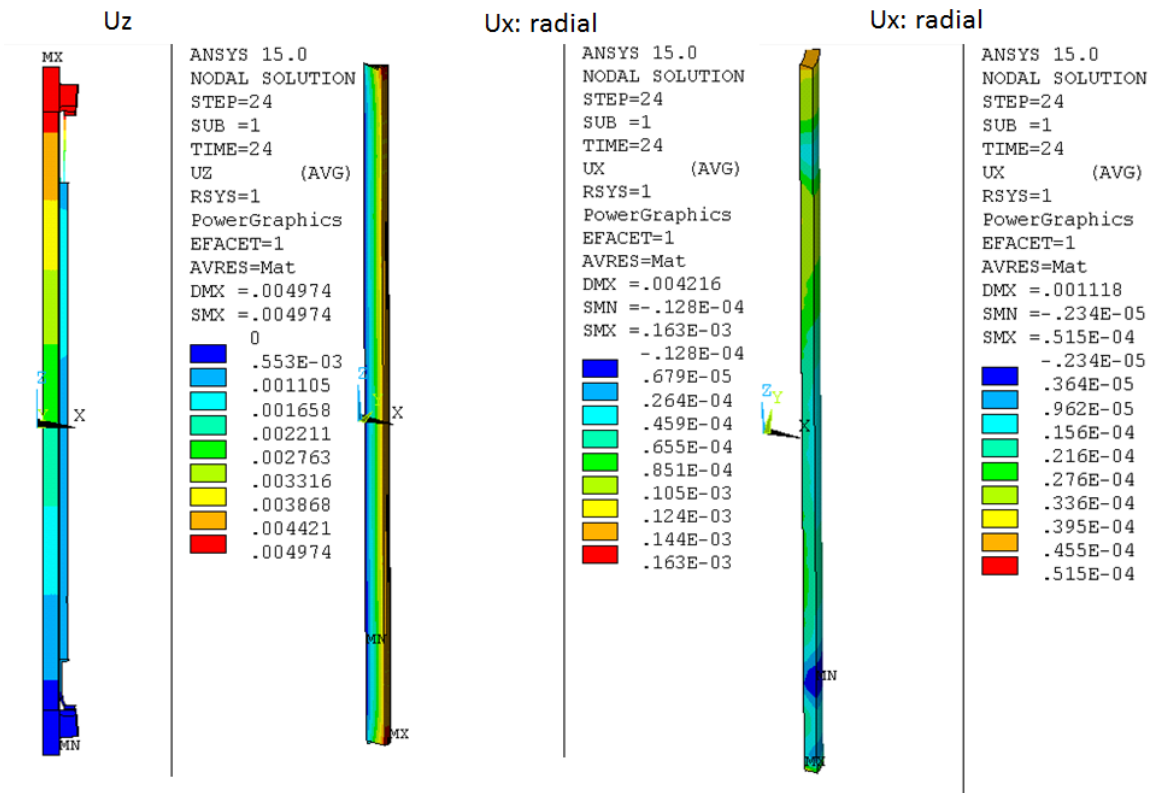


Figure 11.2-6 OH Displacements

Scenario 1 data was used: Sz tension stress

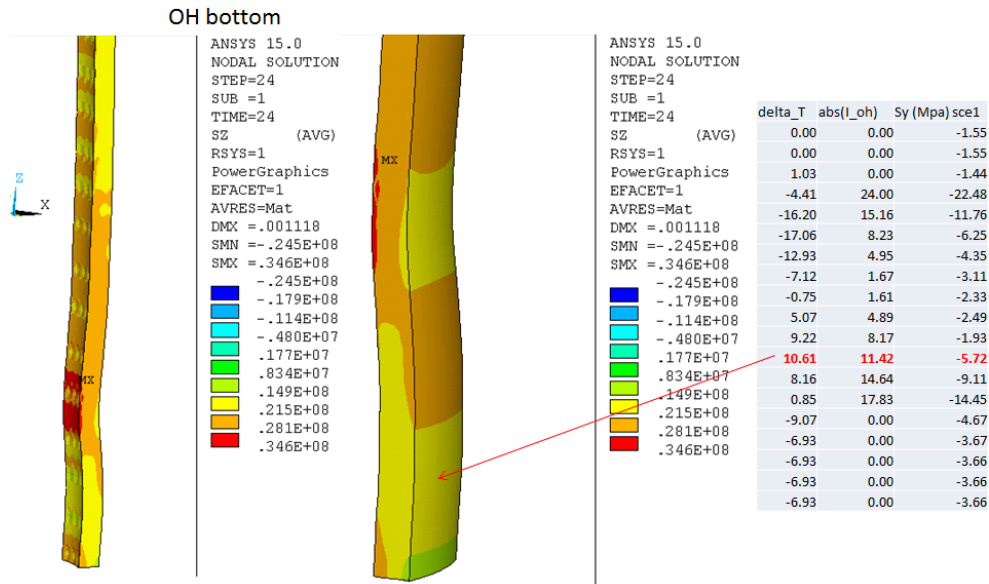


Figure 11.2-7 OH Forces and Displacements

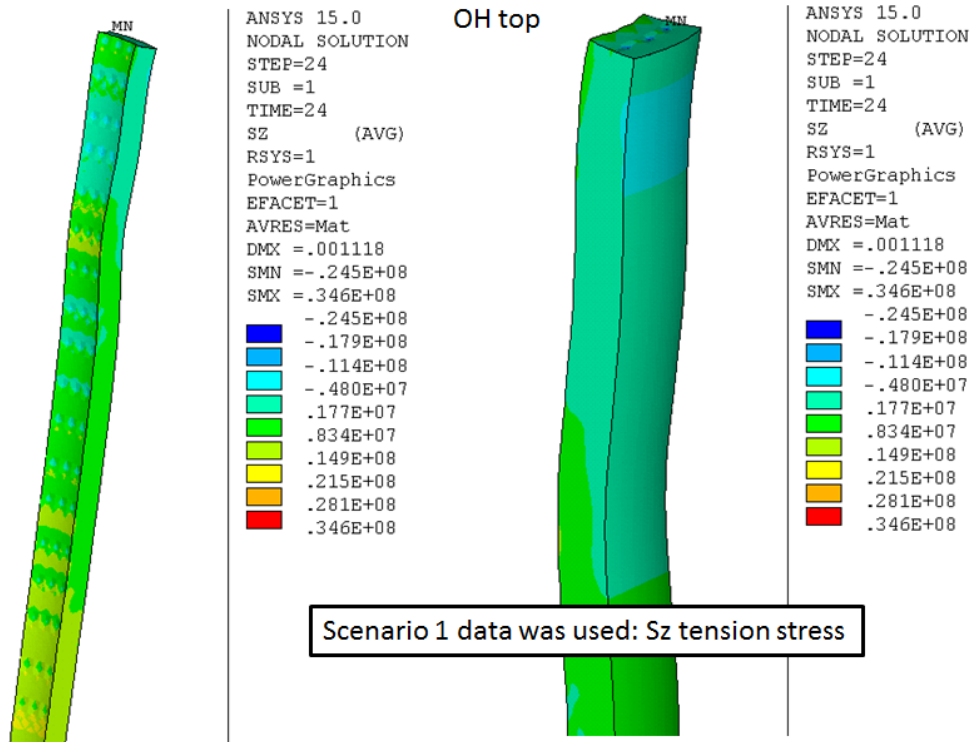


Figure 11.2-8 OH Hoop Stress

12.0 Electrostatic Analysis of Wires Trapped in the Aquapour

Four axial running wires are trapped in the Aquapour that remains between the TF and OH. Attempts were made to use these wires to remove the Aquapour, but this failed and one of the four wires broke in the process. The remaining ends were terminated and insulated as shown in figure 12.0-2.

- Wire diameter is small (~50 mil) leading to possible concentration of electric field due to voltage difference between grounded wire and OH (at 6077 v) and/or TF (at 1013 v)
- Concern is possible breakdown over time of G10 groundwrap insulation on OH or TF
- ANSYS 2D Electrostatic model use to determine max E field
- Results show $E_{max} = 3.5 \text{ MV/m}$
 - Dielectric Strength of Air is $\sim 3 \text{ MV/m}$
 - Dielectric Strength of G10 is $\sim 30 \text{ MV/m}$
- Suggests Insulation offers adequate protection but any air voids could lead to local degradation (Partial Discharges?)

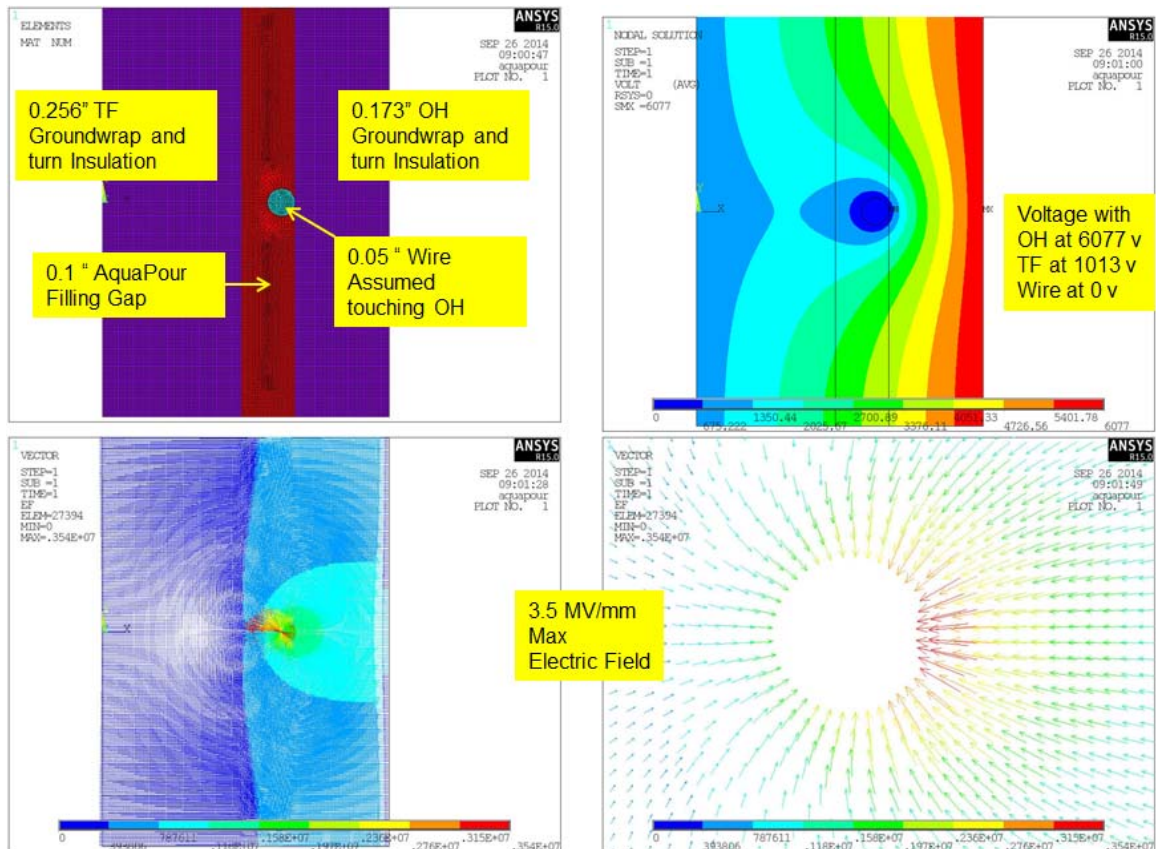


Figure 12.0-1 Results of Electrostatic Analysis of the embedded wires

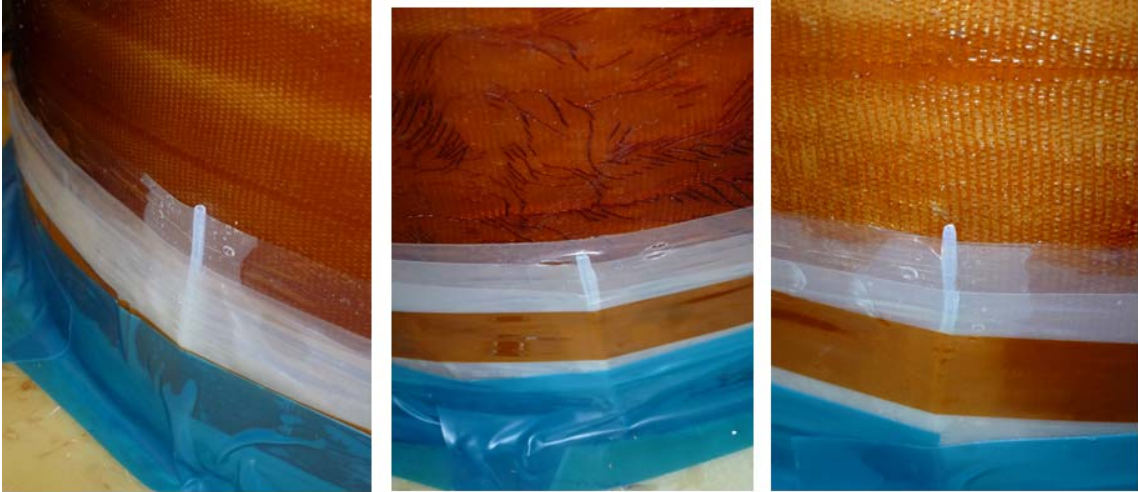


Figure 12.0-2 Termination details of the wires

Steve Raftopoulos provided pictures of the wire terminations in an email dated June 10, 2015. The exposed section (above the OH) of the stainless wires were encapsulated with 2 layers of heavy-dust shrink wrap and then covered with a wet layup of glass tape with Hysol (see Figure 12.0-2).

Electrical Hi Pot Test of OH Coil

Details of the OH coil electrical hi pot test were requested during the review. The photo below shows the center stack during the test. The TF turns were connected together and grounded, the foil over-wrap over the OH coil was grounded, the structure was grounded, and the (4) wires embedded in the Aquapour were grounded. The leakage current from the OH coil to ground was $12\mu\text{A}$ at 13 kV after 1 min.

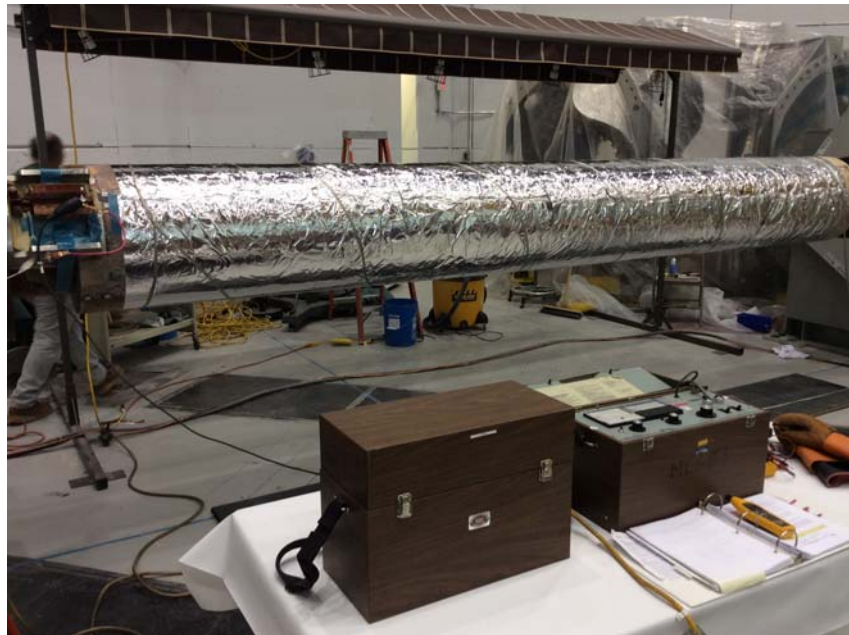


Figure 12.0-3 OH Hipot set-up

13.0 Tests of “AquaCement” Material

If left in the annular space between the OH and TF, the aquacement material should either be sturdy enough to stay in place or weak enough that it would crumble benignly over time. The material appeared very strong to the technicians who were attempting to remove it, so the strength of the material needs to be demonstrated to show that it will remain in place and present minimal problems during operation. Compression tests were requested, and the material is like a strong cement with a low enough modulus that it will not be stressed significantly by the strains of the TF coil.

Pete,

Steve J. called in the first two sample test results for the CTD 425 impregnated Aquapour:

Sample #2:

1.215 x 1.257 x 1.300 " Tall

Failed in compression at 5689 #

Sample #3:

1.225 x 1.242 x 1.320" Tall

Failed in compression at 5794 #

He said it failed like concrete in the tester.

Larry

Email from S. Raftopoulos Attachments 12/9/14 to me, Larry, Erik, Stephan, Ronald load/displacement data from the first two compression tests plotted as stress/strain curve.

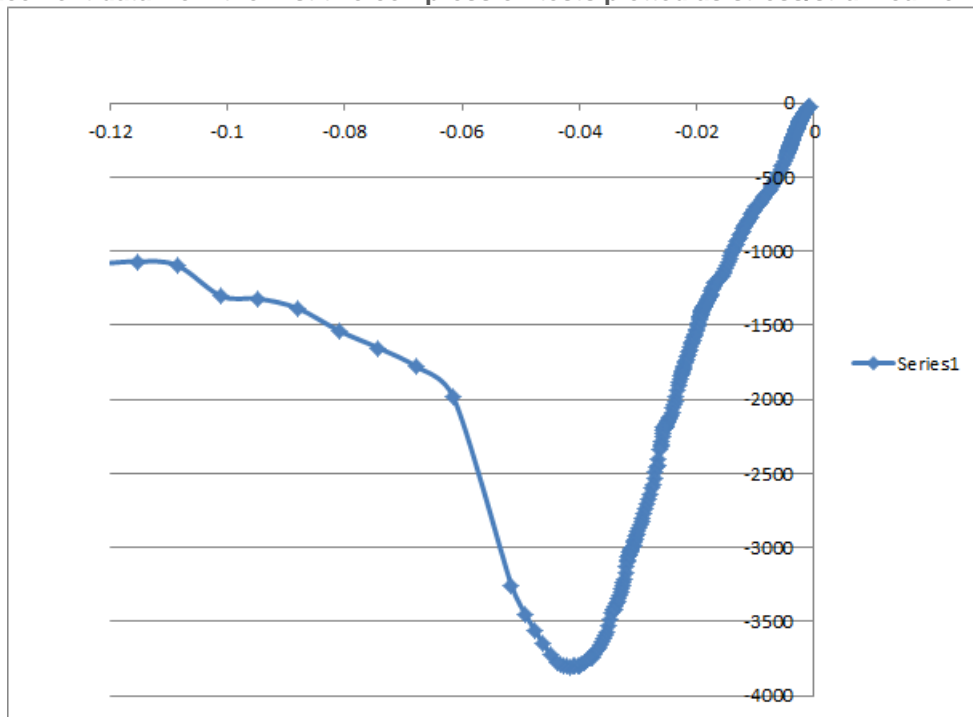


Figure 13.0-1 Force Deflection Measured Data

The modulus is $3750 / (.045 / 1.25) = 104166$ psi or .0075 of copper, which means that glued to the TF, it would experience .0075* TF stresses which are ~30 MPa, so the aquacement stress is tiny. It should not crack or separate. The mechanical design of the OH support is such that it will be difficult for crushed Aquapour to escape. Despite this, periodic inspections at the base of the annular gap between TF and OH, for dust or aquacement chips, are recommended.



Figure 13.0-2 Lower OH Support Area – There Aren't Cracks or Open Areas for powdered Aquapour to Escape

14.0 Array Tensile Test Samples/ CTD Tensile Strain Tests

If the OH is frictionally connected to the TF, it will have the TF strains imposed on it. This is a strain controlled situation in which the OH follows the motion of the TF. To properly test the OH winding pack for this condition, a load controlled test is inappropriate. CTD was contracted to perform strain controlled tests. The testing machine must be set up for displacement controlled tests. The backlash and strains in the load train can be more significant than the test strains. Clip gauges or extensometers are used to control the motions imposed by the testing machine.

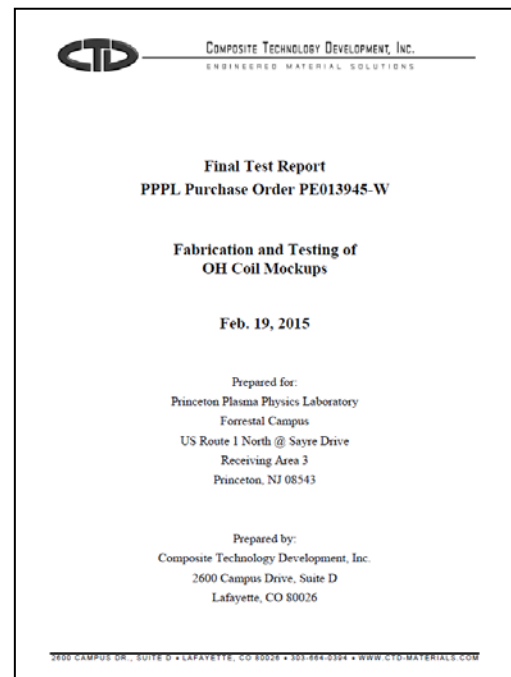
Test Plan Elements:

Test One Aligned and One Misaligned Sample, Load -Deflection, Establish Stiffness/Modulus , onset of cracking and non-linearity, upper bound strength.

Decide on the need for more samples and fatigue testing.

Establish tensile strains for a range of delta T's between TF and OH by analysis.

Perform strain controlled fatigue with electrical performance as the acceptance criteria



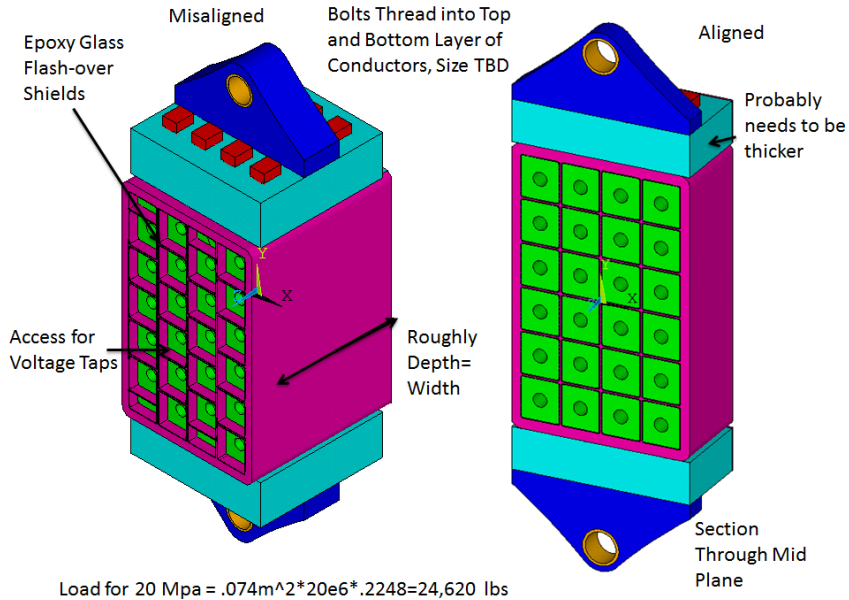


Figure 14.0-1 Proposed Samples, Aligned and Misaligned.

The samples shown in figure 14.0-1 showed the misaligned concept with the flash shield extension (on the left) and a section through the middle of the aligned sample on the right. The concern this test is addressing is whether the turn-to-turn insulation will be damaged by the tensile strain. The ground wrap stays intact and has acceptable stress in the simulations. Consequently, the voltage applied during the test can be representative of the applied turn-to-turn voltage. The layer to layer voltage occurs where the terminals break out and it can be argued that the vertical or axial tensile strains will have less effect on the radial strains in the insulation which would be effected by the layer-to-layer voltage. This voltage is small enough that the flash shields were not included in the sample.

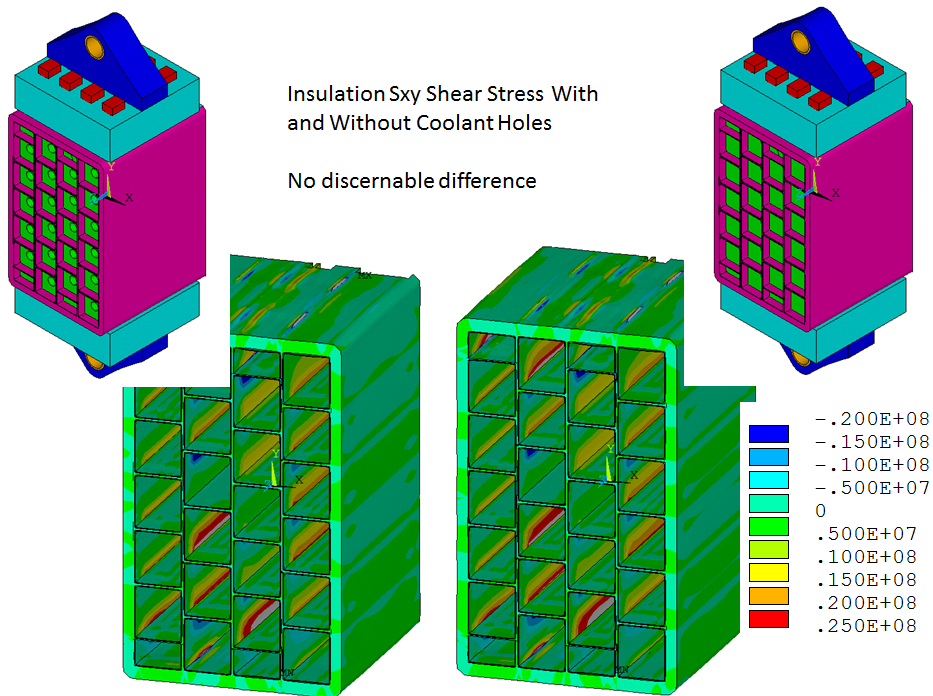


Figure 14.0-2 Sample With and Without Coolant Holes

Models of the proposed samples were analyzed with and without cooling holes. The difference was evaluated by looking at shear stress results at the conductor to turn insulation interface. The difference was very small. This allows simple bar stock to be used for the conductor samples. Extra conductor is available, but if it is not needed the spare conductor can be saved for other future uses. This saved money, time and conductor.

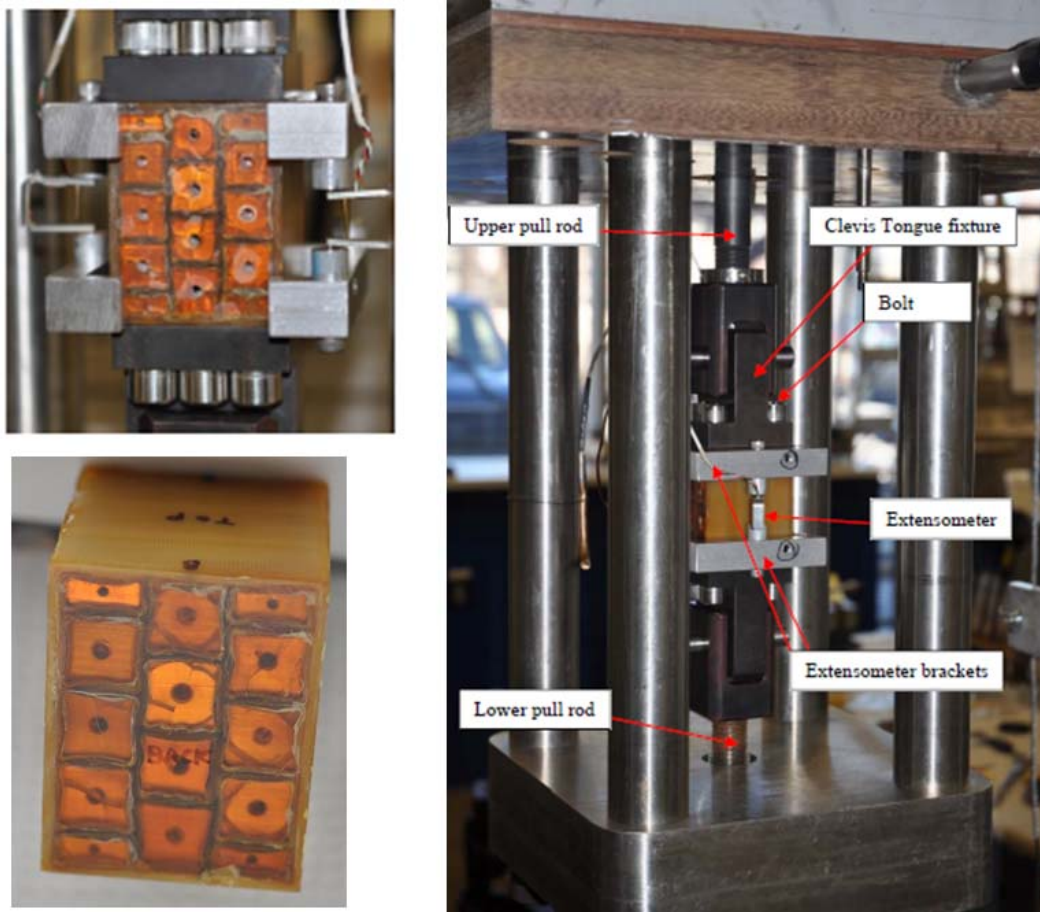


Fig. 14.0-3 Array Test Samples and Fixtures from [25]

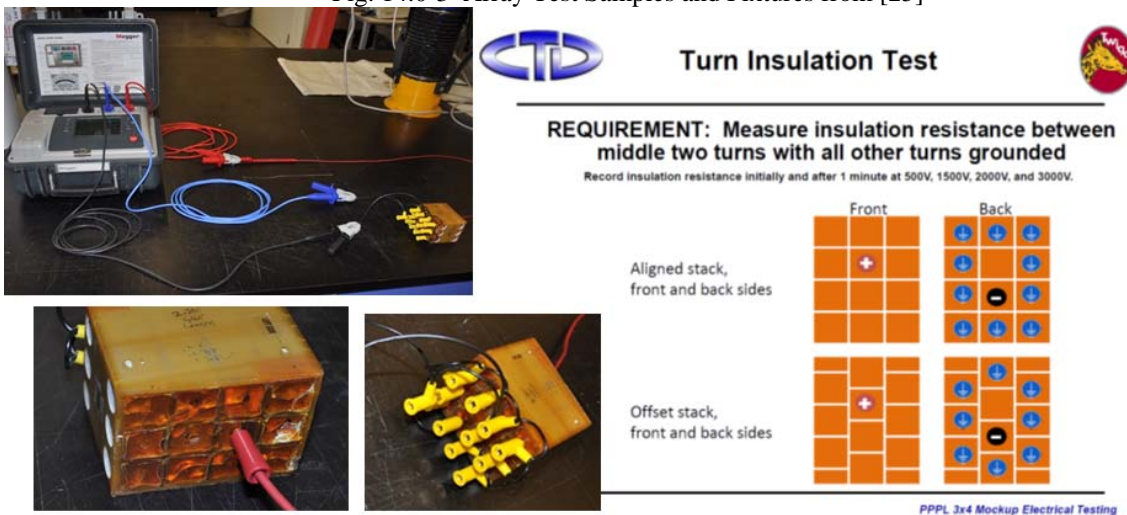


Figure 14.0-4 Test Specimen Electrical Test Setup and Diagram

The CTD array tests show a significant accommodation of tensile strains. The tests are displacement or

strain controlled, performed at 110 C at a strain rate of 0.4×10^{-3} and a rate of ~ 10 hz.

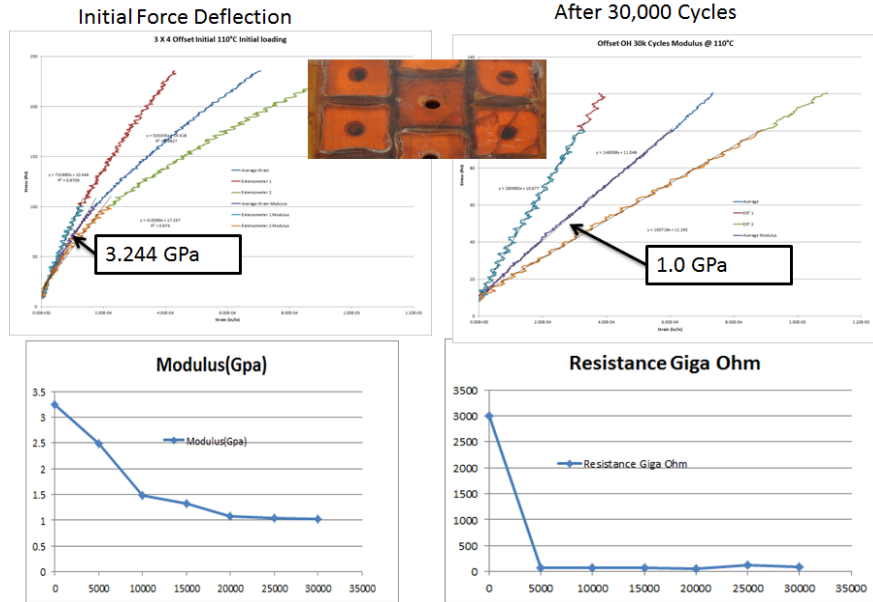


Figure 14.0-5 Moduli and Electrical resistance of the array sample vs load cycle

The measured tensile modulus is surprisingly small.

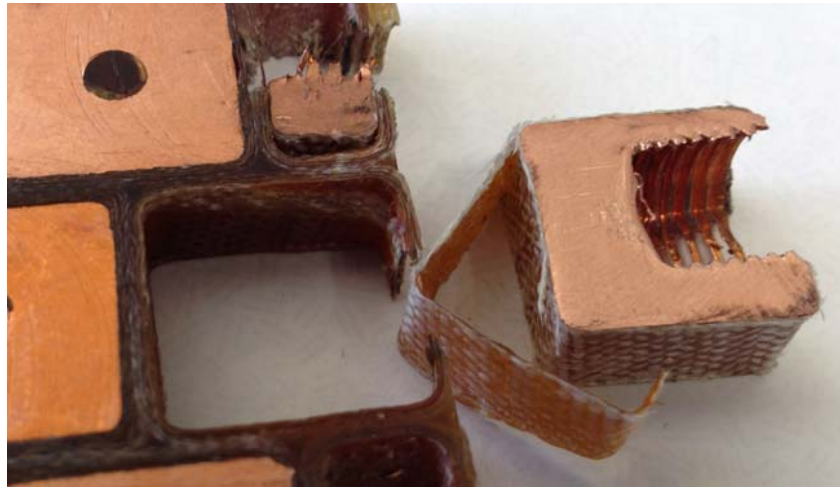


Figure 14.0-6 Separation of one of the conductors by manually pulling on a perimeter conductor

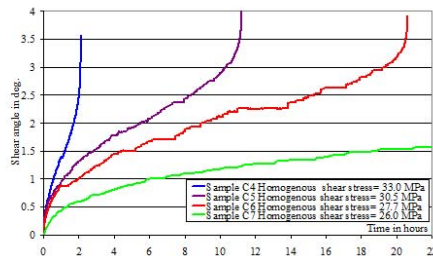
The samples in Figure 14.0-7 do not show any indication of cracking or delamination that is load related. The photos are of the outer faces of the impregnated samples. These are resin rich areas that often crack just from the cooldown from the cure temperature. There is little difference between the two photos of the same sample before and after cyclic testing. The aligned conductor array looks like whatever mechanical change occurs, and this includes the appearance of cracks in the neat resin that occur essentially in the first load cycle. Figure 14.0-6 shows how easily the array comes apart with just manually pulling on one of the conductors. It is clear that the bonds between Kapton and epoxy layers allow separation. The electrical tests show that even with the delamination and de-bonding in the tests, the electrical integrity remains intact. This raises the question as to whether the frictional interaction can be allowed. It is evident that some small level of tensile strains can be allowed, but to quantify this, the simulations of the TF-OH interaction must be predictive and there should be no possibility that axial extensions in the winding pack be allowed to concentrate in one area. The ground wrap probably makes this unlikely, but it is wise at least for initial years of operation, to avoid the frictional interaction.



Fig. 14.0-7 CTD Tensile Strain Controlled Test, Aligned Sample

15.0 Creep Test Sample/CTD Creep Tests

One option to recover all the operating space needed for full performance is to run with elevated OH temperature allowing peak operating temperature above 100 C. For future full performance long pulse inductively driven scenarios, the higher allowable OH temperature would be a help. The current coil temperature limits are set at 100C. 110 to 120C should eliminate interactions between TF and OH for nearly all scenarios. The CTD 425 epoxy system used for the upgrade coils is capable of retaining adequate compressive strength at temperatures above 110 C. Creep behavior might affect retention of preload. The net vertical (launching) load on the coil must be maintained below the preload being applied by a Belleville spring stack at the top of the OH coil. Creep behavior has been tested with a subcontract to Composite Technology Development (CTD).



Results from Gary Voss's Torsion Creep Tester for CTD 403 – The Cyanate Ester

There is noticeable twist even at a couple of hours.

Creep might still occur but the preload mechanism is instrumented and can be adjusted during down times



Figure 15.0-1 Torsional Creep Tests Performed at MAST and the NSTX Preload Mechanism

Figure 15.0-1 introduces the issue of creep loss of preload. Gary Voss measured the torsional creep of the pure Cyanate Ester and found that there was substantial permanent rotation after only a couple of hours at load. A couple of hours seems short, but for 20,000 five second pulses for NSTX-U, in which only about the last second is at full temperature, the total time at temperature and load is 5.5 hrs. The NSTX-U OH sees almost no torsion, only compression, and most shots see the peak compression early in the pulse when the temperature is low.

CTD was contracted to do the creep tests. The sample was a stack of 10 insulation layers, with a copper sheet between each layer, with the whole stack VPI'd together. The width and depth of the column of layers was large

enough to avoid buckling at at least 20 times the layer thickness. The load was 30 MPa compression normal to the layers. This represents the compressive stress in the OH due to the solenoidal self-load. The preload from the Bellevilles is much lower, only 2 MPa and is not expected to contribute to the creep behavior of NSTX-U. Insulation was the same half-lapped Kapton/glass system using the CTD 425 system including primer. The stack was VPI'ed with steel platens on top and bottom, so there is no platen-to-insulation irregular contact. There are 10 layers of insulation in the test.

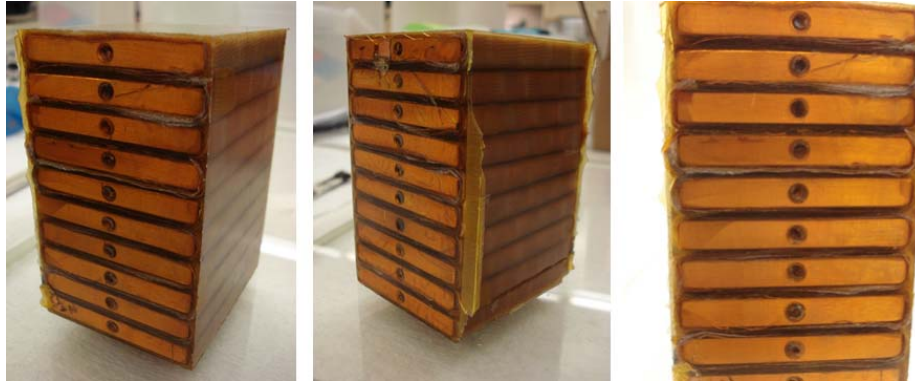


Figure 15.0-2 CTD Creep Stack Test

The sample was first held at 120C and 30 MPa compression for 24 hrs with the stack height measured five minutes after the first application of temperature and compression, then again at 6 hrs, 12 hrs and 24 hrs. If the change in stack height after 24 hrs was more than .05%, then the test was to be repeated at 110C with a new sample. CTD then performed electrical tests on samples to verify the creep behavior of the CTD-425 system had not degraded under load. This test was also used to quantify the modulus for the OH coil. The stresses imposed on the insulation during the Aquapour interaction between the TF and OH are displacement controlled, and thus, are a function of the modulus of the coil winding pack. The load applied by the Belleville springs is set at assembly, nominally with 17.87 mm compression of the stack. This is relaxed when the OH is energized and shrinks due to self-load. It is also relaxed over time if creep effects are significant. The load remaining in the Belleville stacks must offset any launching load on the OH due to interactions with the other PF coils. The uncertainty in the modulus dictated a conservatively stiff modulus for an upper bound on stresses. In this section, a reasonable modulus for analysis of minimum preload will be developed.

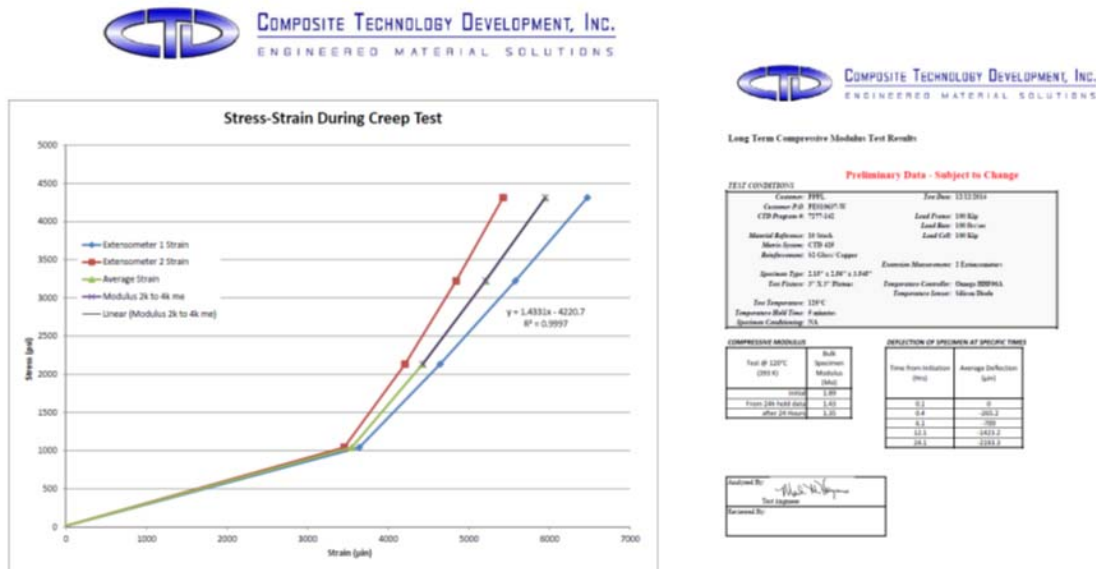


Figure 15.1-3 CTD Load Deflection Curves for the Creep Test Specimen

The slope of the curves after “squeezing the air out of the load train” is $(4250-1000)/(6000e-6-3500e-6) = 1.3e6$ psi. This is for 10 insulation layers. The displacement for the 10 layers is .008863 inches. This is calculated from the sample stack height of 3.545 inches and a strain range (.006-.0035). For 222 turns in a layer and a height of the OH of 4.206 meter, the effective modulus would be:

$3250/(0.008863*222/10/(4.206*39.37))= 2.735e6$ psi = $18.8e9$ Pa. Very low. This is for fully aligned conductors, but it still looks suspect compared with computed moduli. This could be backlash or fit-up issues with the platens, maybe lack of fill in the interlayers of the lapped Kapton, or the epoxy itself is softer than assumed in the analysis. The OH preload mechanism is instrumented and during early stages of the NSTX start-up, the change in OH height, when energized, has been measured and this gives a direct indication of the OH winding pack modulus.

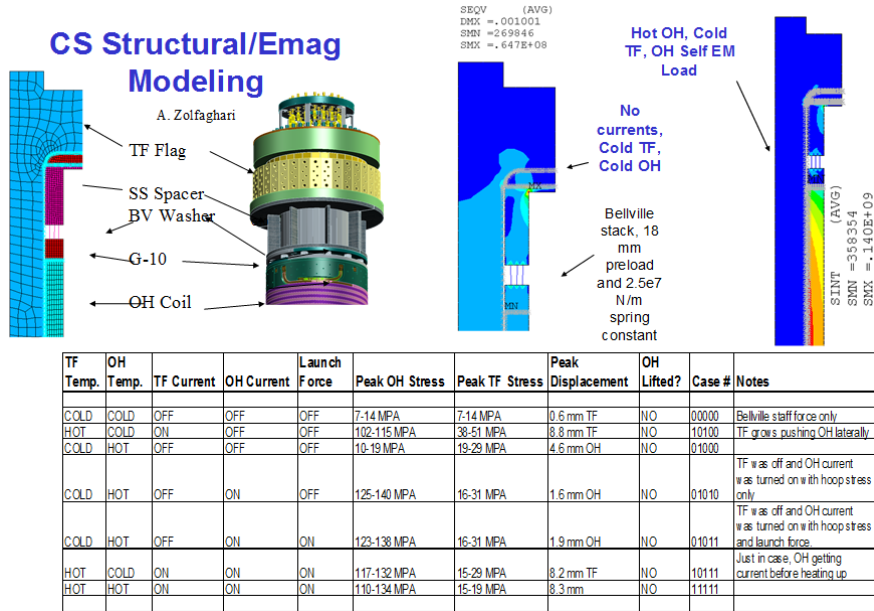


Figure 15.1-4

The table/figure below (Figure 15.1-5) is from Peter Rogoff’s calculation, NSTX CALC 133-04[10]. The nominal range is: $23.87-9.47 = 14.4$ mm. Since we are trying to model some degree of unexpected displacements, it is recommended that an LVDT be purchased that can measure at least 2 cm.

If the LVDT is zeroed when the preload is imposed, then the LVDT would have to measure:

$(17.87-9.47) =$ (plus) 8.4 mm (When the TF is hot and the OH is cold)

$(17.87-23.87) =$ (minus) 6 mm (When the OH is hot and the TF is cold)

$(8.4-6.0) =$ (plus) 2.4 mm (When the TF is hot and the OH is also hot)

Performance Summary						
And						
Input to digital coil protection system						
System scenario	Compression mm	Force on OH N	Force on OH lbs.*	Tensile Stress N/mm	Fatigue Cycles	
NSIX OH Preload System and Bellville Springs	Pre Load	17.87	162,512	36,520.	849.	-----
NSIX-C-6C-214449 Rev 0 October 2010	TF hot OH hot	15.47	142,268.	31,970.	731.	2 Mil. +
Prepared By: Peter Rogoff Senior Engineer Power Dept. PPE, Mechanical Engineering	TF hot OH cold	9.47	89,698.	20,157.	459.	high
Reviewed By: Thomas Kozub Senior Engineer Power Dept. PPE, Mechanical Engineering	TF cold OH hot	23.87	211,582.	47,546.	1185.	500,000
Reviewed By: Peter Titus Senior Engineer Power Dept. PPE, Mechanical Engineering	Thermal expansions: FT = 8.4 mm OH = 6.0 mm					
Power Dept. PPE, Mechanical Engineering Analysis Division				* Allowable OH launching loads. Note: For supporting calculation see power point files for full details.		

Figure 15.1-5 Preload Table from [10]

The first indication we will have of a variation in the design parameters will be if the preload system jacking screws have to be tightened more than the nominal compression of 17.87 mm to actually achieve the desired 17.87 mm of Belleville spring stack compressive displacement. They should be almost one-to-one, i.e., for reasonable moduli, the elastic behavior should be very small compared with the thermal displacements. The preload elastic coil displacements are ~1/10 mm, Lorentz displacements are ~ 1 mm.

From reference [8] section 7.1.1, the winding pack radial and vertical composite moduli were computed to be ~85 MPa. Models by Zolfaghari, Zhang and Brooks, as well as Titus unit cell analyses (above) show similar behavior above that of the CTD test. There will be a number of opportunities to benchmark the axial modulus of the coil. CTD will provide results for the array samples – both aligned and misaligned, as well as for the creep samples. The best indication of the coil modulus will be from LVDT readings from the OH Belleville preload mechanism.

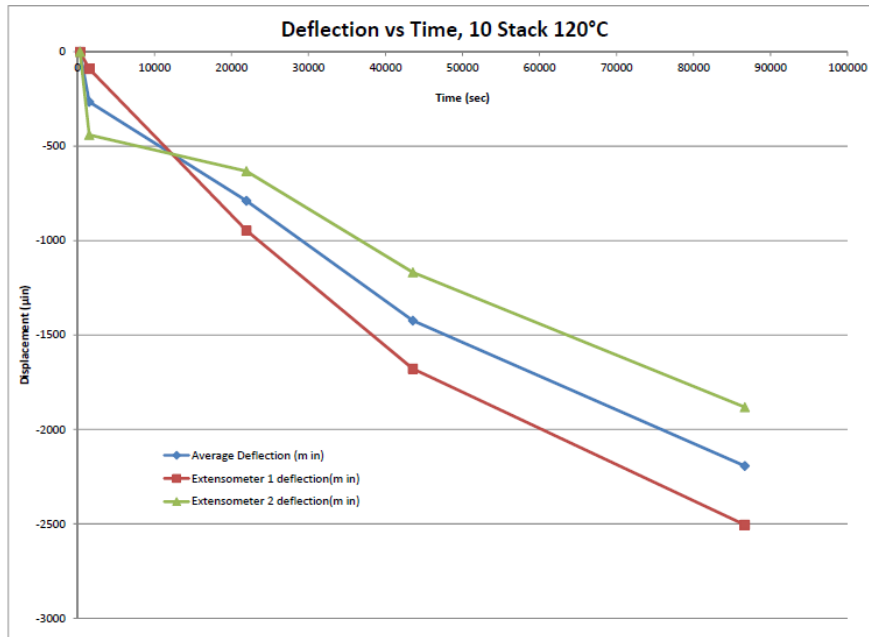


Figure 15.1-6 Deflection vs. Time for the Creep Test at 120C

The preliminary CTD results show about 2,200 microstrain after 85,000 seconds. This is for 10 insulation layers, so the total displacement for the stack of 10 interfaces is:

The stack height = 3.545 inches. With a strain change = 2200×10^{-6} , the dimensional change of the sample is .0078 in. For 222 turns in a layer, the displacement of the coil due to creep is $.0078 \text{ in} \times 222 / 10 = .173 \text{ in}$ (4.3 mm).

For 110 degrees, the permanent change in height is .005 and a height of the OH of 4.206 meter, the effective modulus would be: $3250 / (.008863 \times 222 / 10 / (4.206 \times 39.37)) = 2.735 \times 10^6 \text{ psi} = 18.8 \times 10^9 \text{ Pa}$. Very low.

As of June 2015, we have data from the LVDT mounted on the preload mechanism.

#1 pc_fiso10V_ch1 NE OH Upr Pre-Load

#2 pc_fiso10V_ch2 SE OH Upr Pre-Load

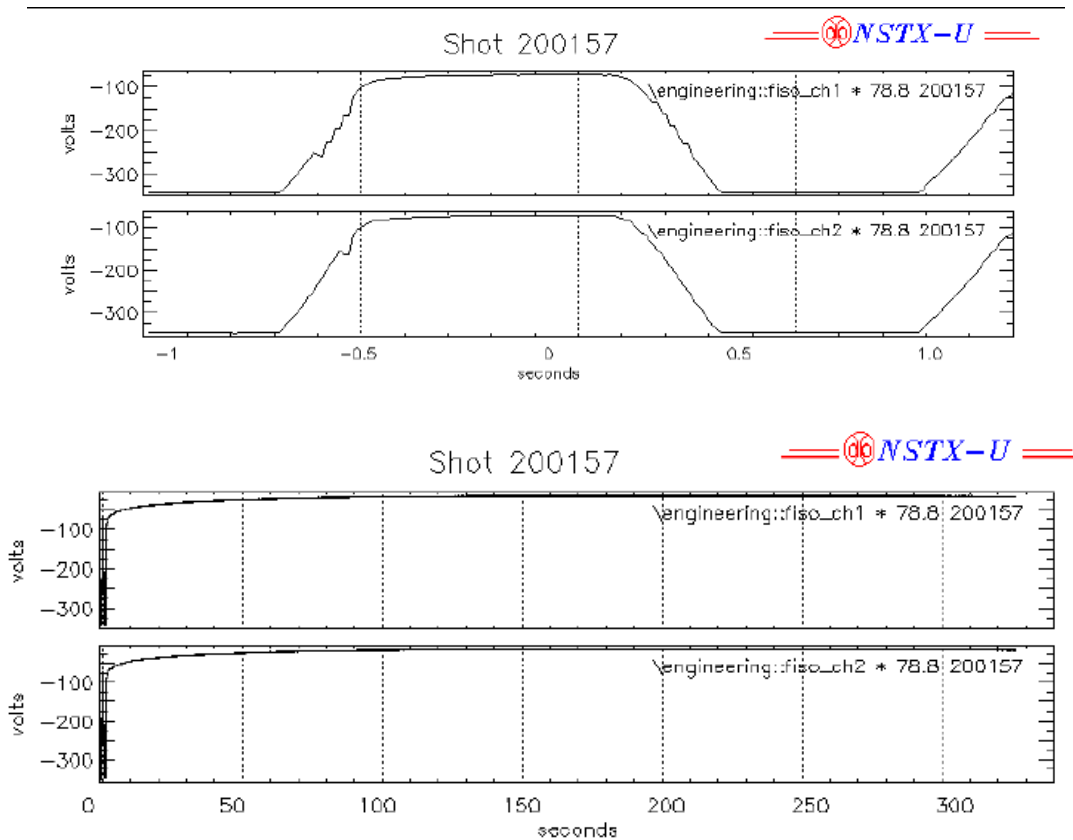


Figure 15.1-6 Combined Shot, TF and OH

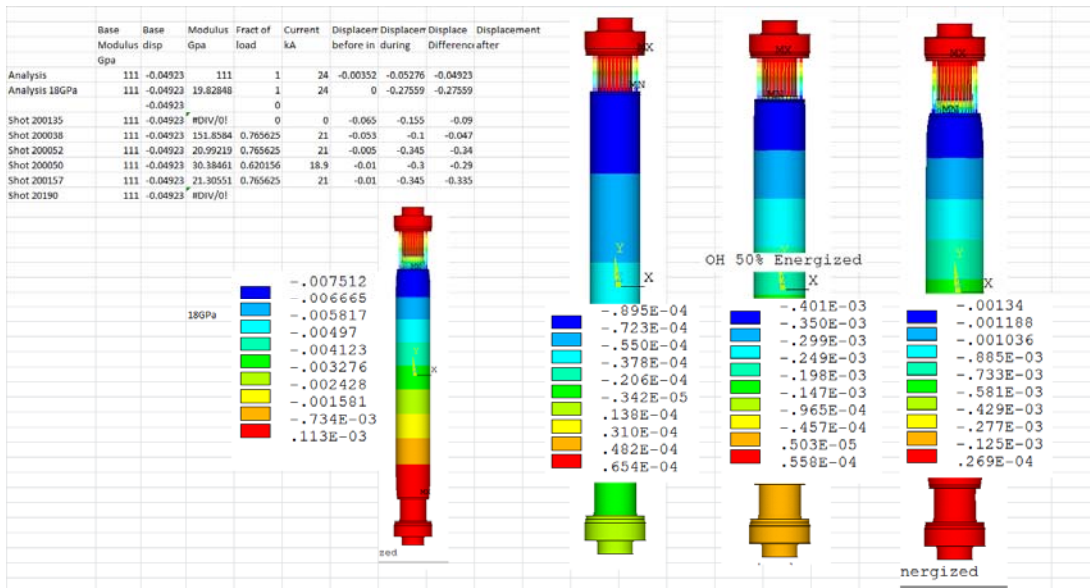


Figure 15.1-7 Calculations Based on Measured Displacements During April 2015 Run

Figure 15.1-7 shows the estimate of the modulus from measured LVDT data. This was used to estimate the preload force and the expected range of force vs. LVDT displacement. From the creep stack test, the modulus was estimated to be 18.8 GPa and the measured LVDT data produced 20 to 30 GPa. So it is much lower than mixture rule estimates.

Allowed Launching Load vs. LVDT Reading (m), Based on .007m OH Compression at 24 kA
OH and TF temperatures are varied. OH current held at 24kA

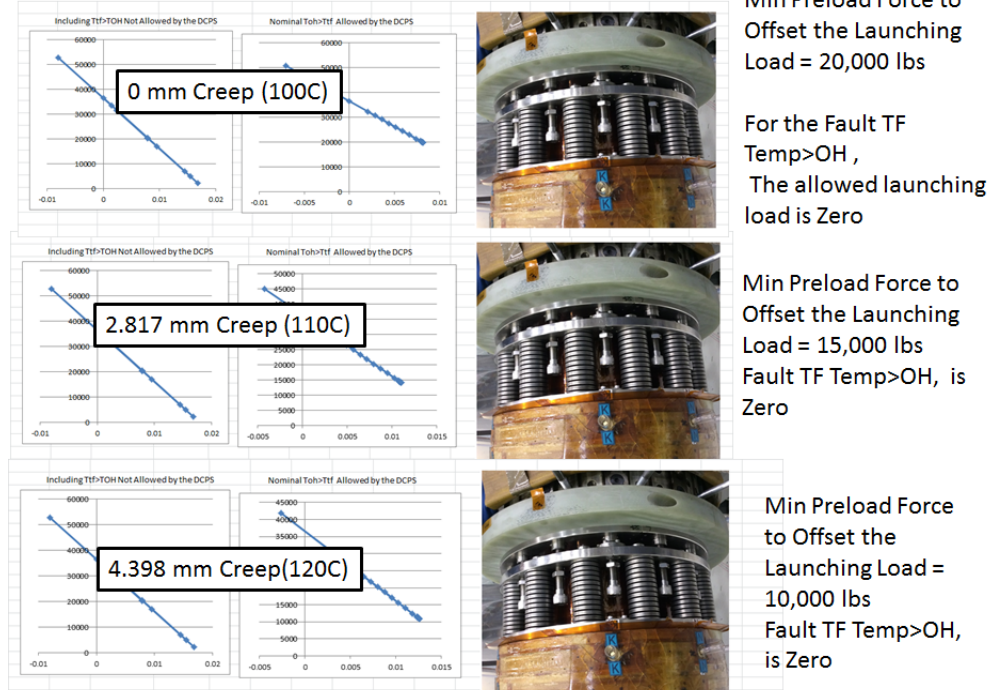


Figure 15.1-8 Preload Compression vs Displacement as Measured by the LVDT for Predicted Creep

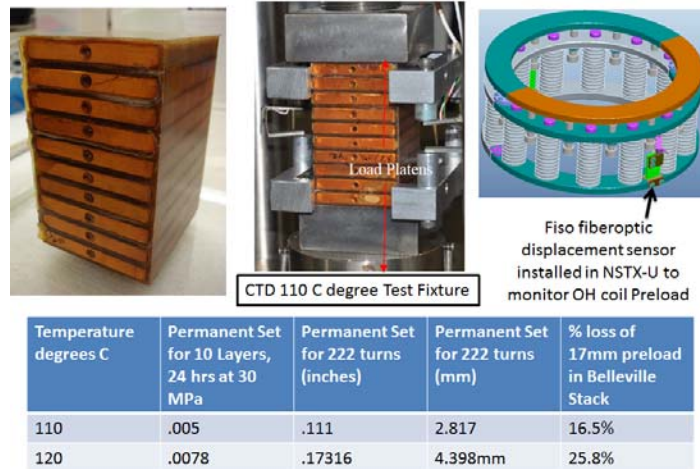


Figure 15.1-9 Preload Loss for Different OH Temperature Limits Based on Creep Measurements

Tests were conducted at 30 MPa compression which is the compressive stress resulting from the self-load of the NSTX-U solenoid when fully energized. Compression from the preload alone is only 2 MPa and is not expected to contribute to the creep behavior of NSTX-U. Creep tests were performed by Composite Technology Development (CTD) [12]. The compression in the test was maintained for 24 hours. The sample, test fixture, and preload mechanism are shown in Figure 15.1-9.

Creep is a function of time at temperature and load. The 30 MPa compression results from the solenoidal self-load at full energization. It lasts for only fractions of the 5 second pulse – maybe 1 second at the precharge and another second at the bottom end of the swing. The cooldown time for the OH is 20 minutes with the lower end of the coil remaining hot for about 5 minutes and the upper end of the coil hot for the full 20 minutes, until the cooling wave exits. Based on time at concurrent load and temperature, the 24 hr test represents ~ 43200 shots above the 20,000 full power shots specified for NSTX-U. Measured creep was linear in time during the test and has been scaled down to the 20,000 shot requirement in Figure 15.1-9. The preload will be monitored through NSTX-U operation with Fiso displacement sensors. These are fiberoptic based and are not affected by magnetic fields, so preloads during the shot, and over many shots can be monitored.

Creep displacement of the winding pack for normal operation of NSTX-U at 110 C appears manageable. However, the measured modulus of the sample was lower than that calculated from the mixture rule and the winding pack geometry. This is estimated to be only 19 MPa vs. 65 MPa used in the initial sizing of the OH coil and its preload mechanism.

Creep effects will have to be monitored using the LVDT instrumentation installed on the Preload mechanism. The preload mechanism is adjustable and compression in the Belleville stack can be improved in future years if creep is a factor.

Permanent Aquapour/CTD-425 Composite Does Have Some Advantages

- OH coil will stay well centered on the TF bundle.
 - Eliminates the need for centering shims.
- OH pre-load mechanism is more robust.
 - OH pre-load provided by Belleville washer stack pushing on the TF coil flags.
 - 20 klb limit on the OH F_z determined by the hot-TF, cold-OH case.
 - By eliminating this case, the F_z limit is increased to 30 klb.
 - Provides additional headroom for control oscillations.

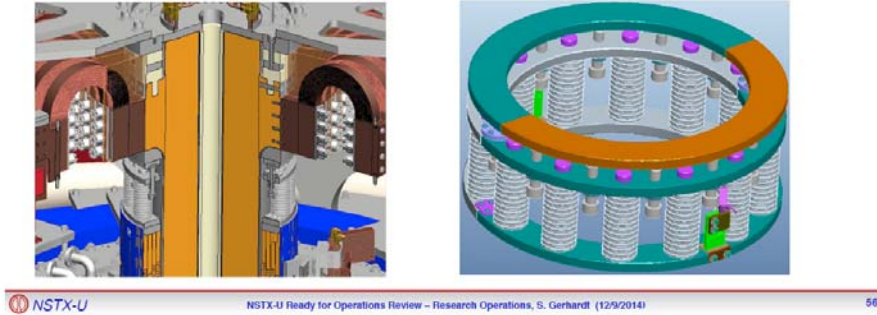


Figure 15.1-10 “Advantages” of the Aquapour


Figure 15.1-10 is from a presentation by Stefan Gerhardt discussing the “advantages” of leaving aquapour in place. It was intended as a facetious remark, but figure 15.1-8 shows the minimum allowed launching load that results from the more compliant OH. If the TF were allowed to go warmer than the OH, the launching load limit would go below the 20,000 lbs currently coded into the DCPS.

Reference 5 These are the “Bad” Scenarios

Stefan Gerhardt (via Google Drive) <sgerhard@pppl.gov> 8/8/14


to me
mmarden
jmenard
hzhang
jchrzano
rstrykow
mono

I've shared an item with you.

 [TimeDependentScenarios](#)

These are the “Good” Scenarios

Inbox



Stefan Gerhardt (via Google Drive) <sgerhard@pppl.gov> 9/5/14

to me
mmarden
hzhang
jmenard
tstevens
jchrzano
rstrykow
mono

Images are not displayed. Display images below - Always display images from sgerhard@pppl.gov

TimeDependentScenarios

This has been updated to have a bunch more scenarios...the Pete15 through Pete 19 cases, each of which has a few different instances.

These maintain TOH>TTF all the time, and use a 110 C limit on the OH to get out to 5 sec. in some cases.

TimeDependentScenarios

Email from S. Raftopolis, June 9 2015

The exposed section (above the OH) of the stainless wires were encapsulated with 2 layers of heavy-dust shrink wrap and then covered with a wet layup of glass tape with Hysol. See pics

Pete,

Steve J. called in the first two sample test results for the CTD 425 impregnated Aquapour:

Sample #2:

1.215 x 1.257 x 1.300 " Tall

Failed in compression at 5689 #

Sample #3:

1.225 x 1.242 x 1.320" Tall

Failed in compression at 5794 #

He said it failed like concrete in the tester.

Larry

Email from S. Raftopoulos Attachments12/9/14 to me, Larry, Erik, Stephan, Ronald
load/displacement data from the first two compression tests plotted as stress/strain curve